

Fluoroscopic Navigation for Robot-Assisted Orthopedic Surgery

Cong Gao

Ph.D. Candidate

Department of Computer Science
Johns Hopkins University

1

C-arm Fluoroscopy for Orthopedic Surgery

C-arm is a commonly used machine in most orthopedic operating rooms

- X-ray imaging is fast, low-cost, supplies in-depth structures of the patient anatomy
- Consecutive fluoroscopic shots present intraoperative structure changes

Goal: Guide the surgeon to operate the surgical tool and evaluate the performance



Philips Zenitron C-arm platform^[1]

[1] Image from: <https://www.philips.com/a-w/about/news>

2

Fluoroscopic Guidance Challenges

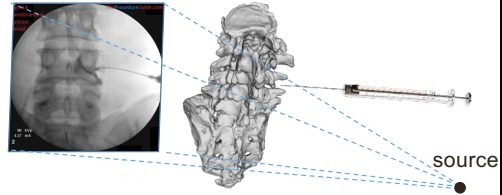


3D information is collapsed in X-ray projective imaging

- The clinicians estimate the critical 3D information through “mentally mapping”
 - Intraoperative tool-to-tissue relationship
 - Relationship with respect to pre-operative planning



Failed estimations can lead to large operation errors



X-ray Transmission Imaging Illustration



Example Spine Needle Injection X-ray^[2]

[2] X-ray image from <https://theprocedureguide.com/fluoroscopic-guided-thoracic-lumbar-transforaminal-epidural-steroid-injection/>



3

Robot-Assisted Orthopedic Surgery

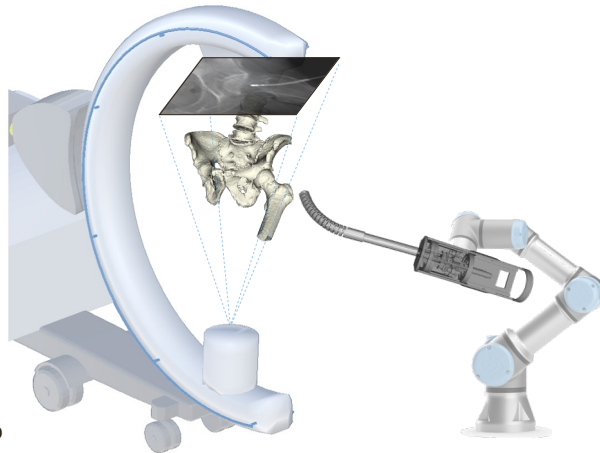


Robotic Surgical System

- Better precision, more stable, safer than human's freehand
- Automates the control of more complicated surgical tools

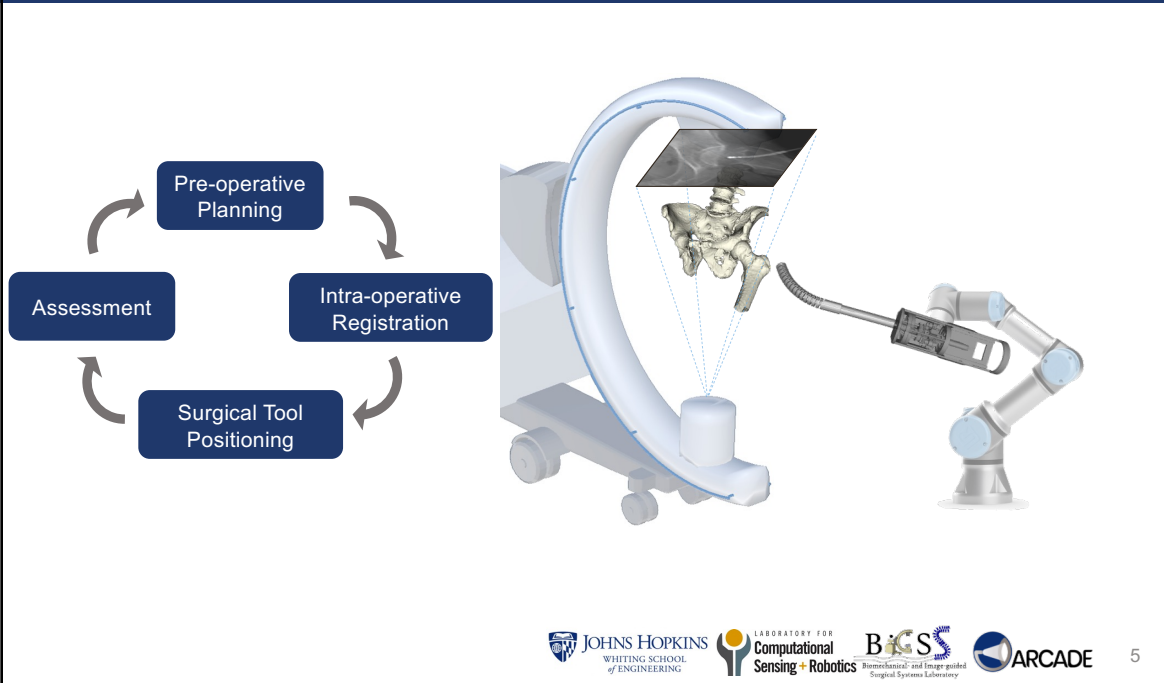
Navigation system is critical

- Quantitatively computes 3D tool to tissue relationship
- Navigates the robotic surgical tool to planning positions



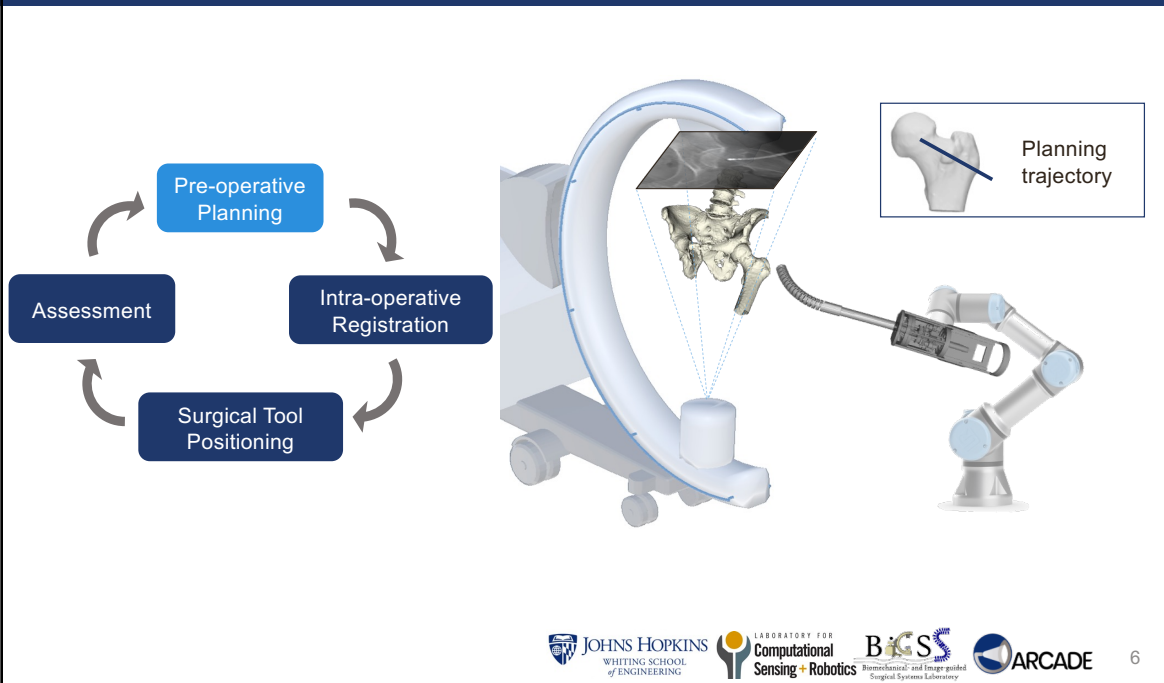
4

Concept of Fluoroscopic Navigation System



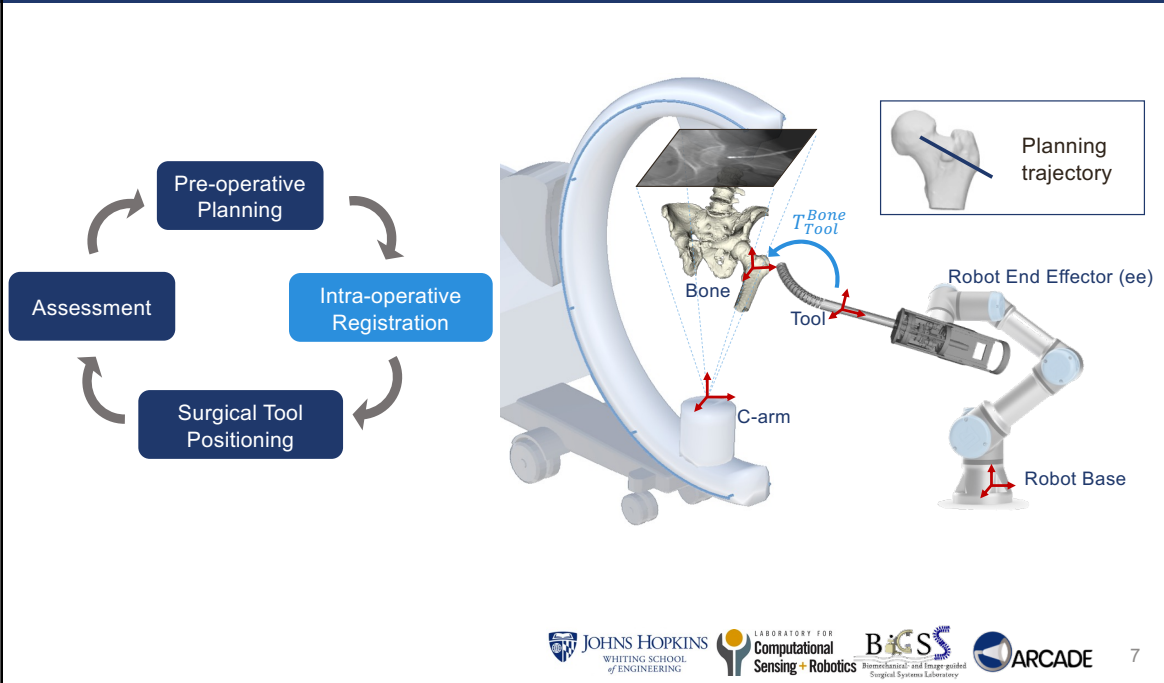
5

Concept of Fluoroscopic Navigation System



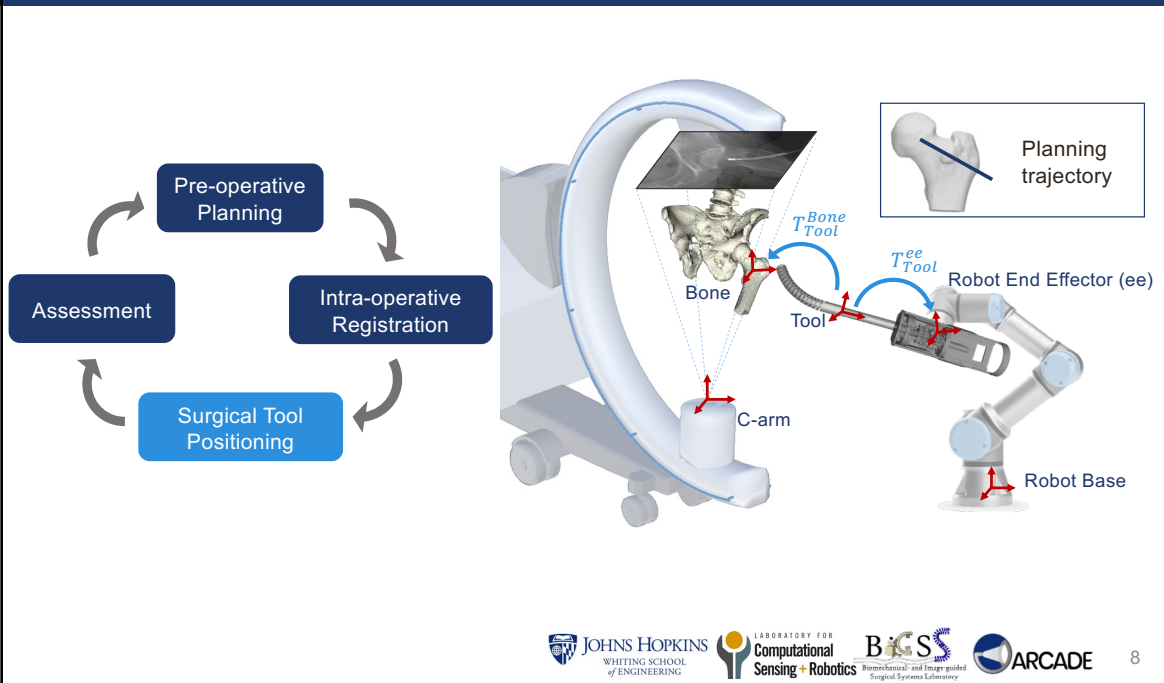
6

Concept of Fluoroscopic Navigation System

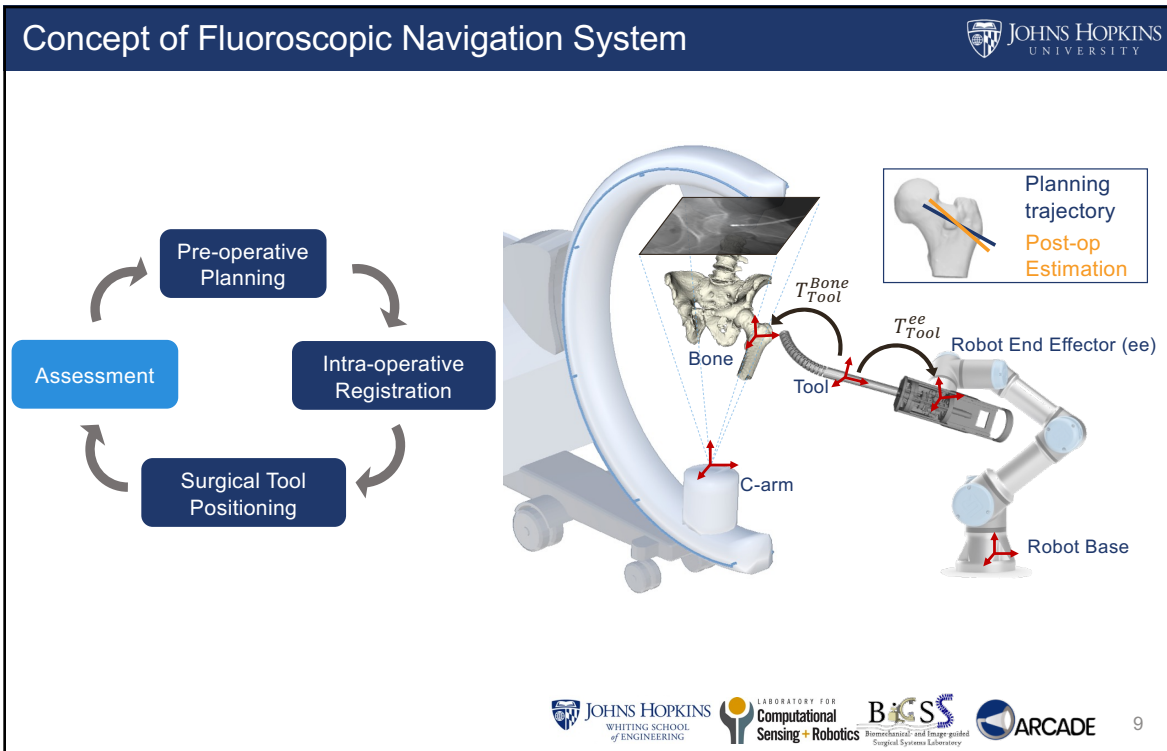


7

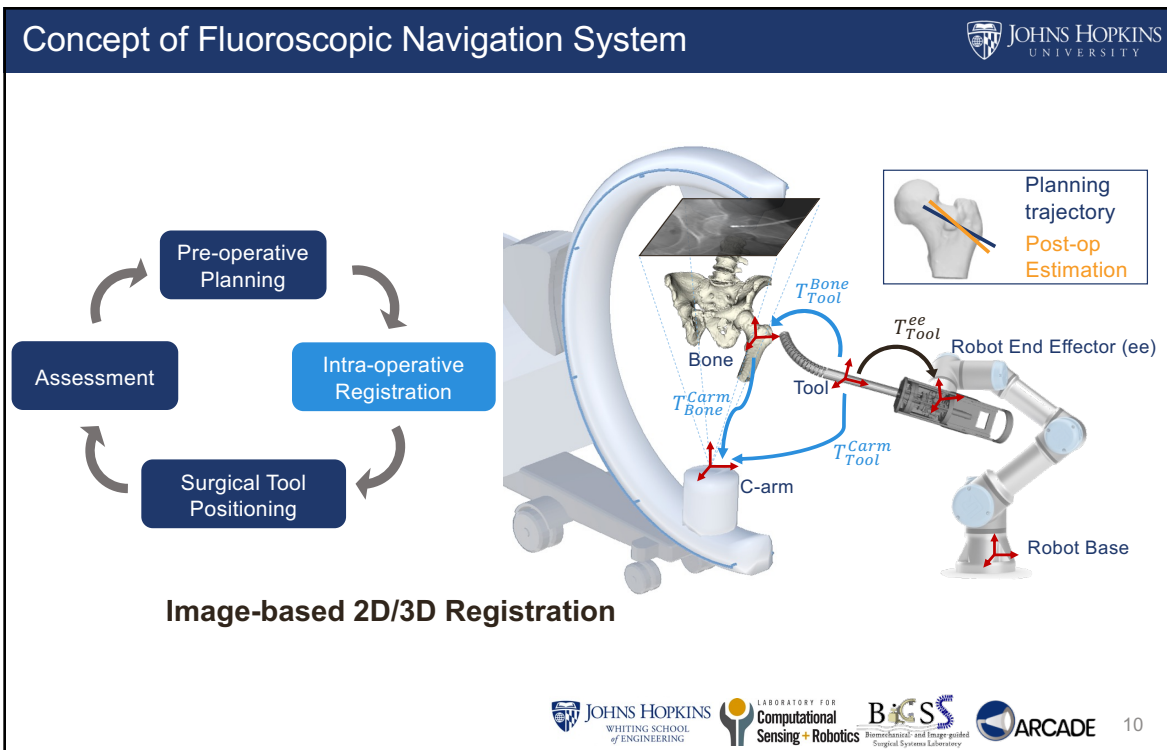
Concept of Fluoroscopic Navigation System



8



9



10

Intra-operative Registration Fundamentals

2D/3D Registration

Given the following:

- 2D target image I_t
- 3D volume V
- pose parameter $\theta \in SE(3)$
- a Digitally Reconstructed Radiography (DRR) operator P
- a similarity function S

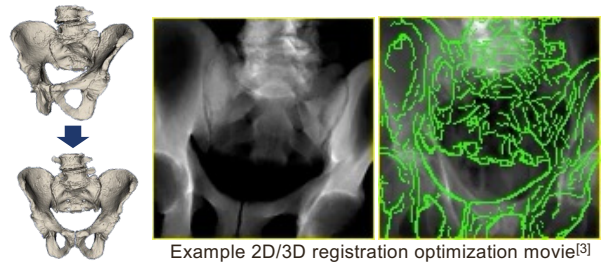
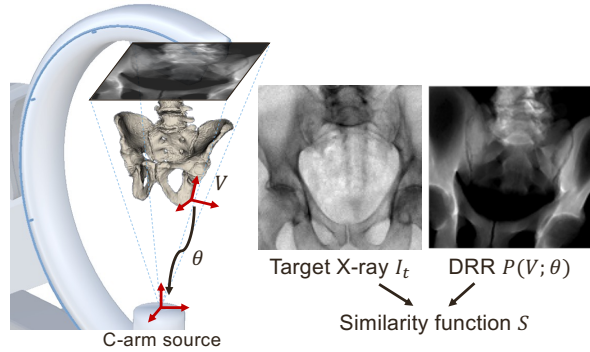
2D/3D Registration solves the following optimization:

$$\theta = \min_{\theta} S(I_t, P(V; \theta))$$

When generalizing to multiple m objects and n images, including pose regularization term R :

$$\{\theta_m\} = \min_{\theta_m} \sum_{n=0}^N S(I_n, P(V_m; \theta_m)) + R(\theta_m)$$

$$m \in \{0, \dots, M\}, n \in \{0, \dots, N\}$$



Example 2D/3D registration optimization movie^[3]

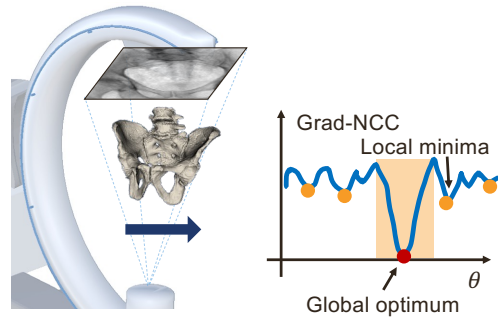
[3] Generated using open-source software: xreg <https://github.com/rp2/xreg>

Challenges

2D/3D Registration Challenges

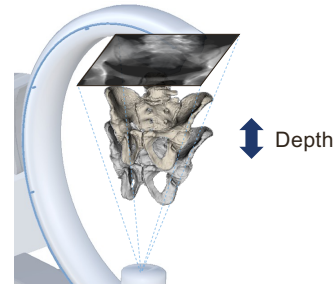
Narrow Capture Range

- Local minima of conventional hand-crafted similarity function, such as Gradient Normalized Cross Correlation (Grad-NCC)
- Requires the initialization close to the ground truth



Ambiguity

- Single-view registration is ambiguous along depth direction due to collapsed information in projective geometry
- More serious if the search space is more complex, such as deformable registration

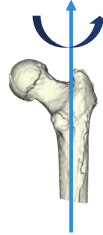


Challenges

Bone Anatomy Registration Challenges:

Proximal Femur

- Lack of distinct features in X-ray image
- Ambiguous in axial rotation

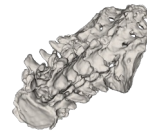


Example X-ray^[4]



Spine Vertebrae

- Multi-component, size is smaller
- Shape deforms intra-operatively



[4] X-ray image resources:

<https://radiopaedia.org/cases/normal-ap-lumbar-spine>

Chiamil, Sara Muñoz, and Claudia Astudillo Abarca. "Imaging of the hip: a systematic approach to the young adult hip." *Muscles, Ligaments and Tendons Journal* 6.3 (2016): 265.

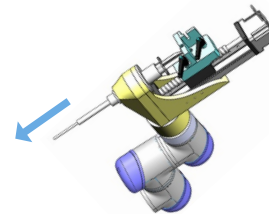
13

Challenges

Surgical Tool Registration Challenges:

Rigid Bone Drilling & Injection Device^[5]

- Metallic guide is symmetric, no texture under X-ray
- Orientation accuracy is critical

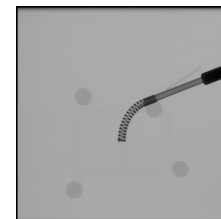
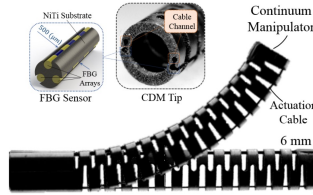


Example X-ray



Dexterous Continuum Manipulator^[6]

- Small and flexible
- Shape estimation is critical



[5] Bakhtiarnejad, M., Gao, C., Farvardin, A., Zhu, G., Yu, W., Oni, J., Taylor, R.H. and Armand, M., 2022. A Surgical Robotic System for Osteoporotic Hip Augmentation: An Early feasibility study. Under Review of TMRB

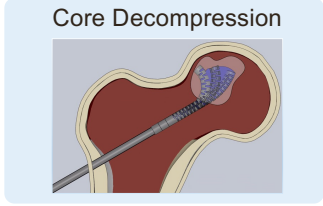
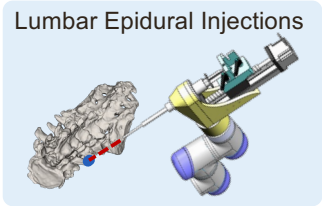
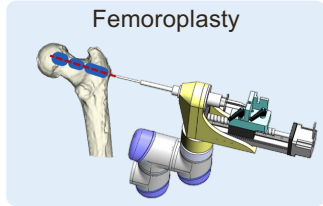
[6] Sefati, S., Hegeman, R., Alambegi, F., Iordachita, I., Kazanzides, P., Khanuja, H., Taylor, R.H. and Armand, M., 2020. A surgical robotic system for treatment of pelvic osteolysis using an FBG-equipped continuum manipulator and flexible instruments. *IEEE/ASME Transactions on Mechatronics*, 26(1), pp.369-380.

14

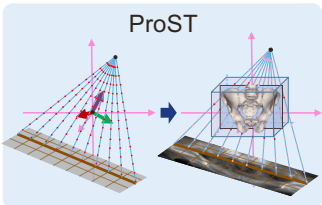
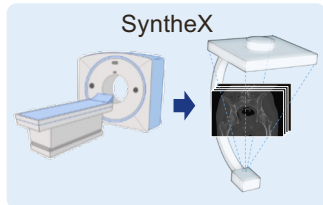
Outline



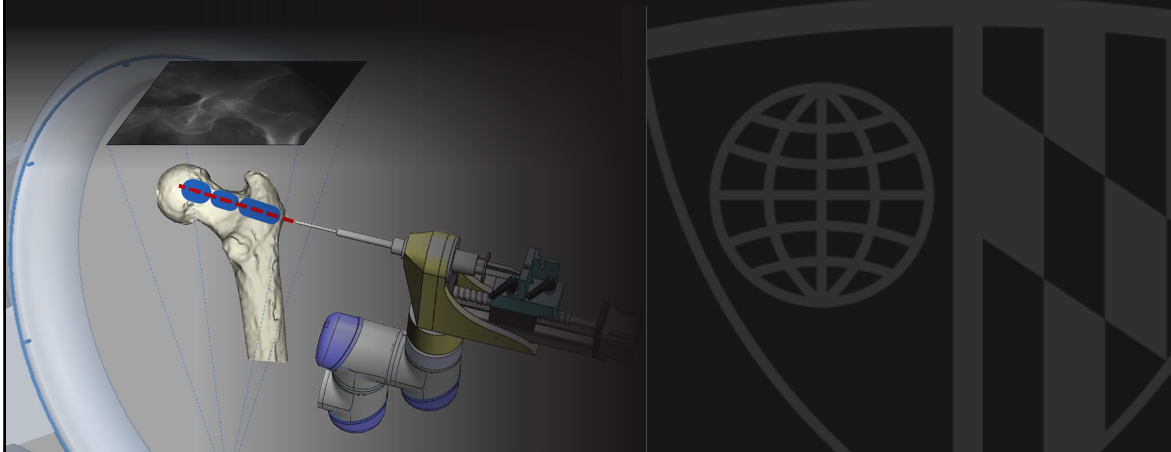
Part I: Clinical Application Developments



Part II: Machine Learning Investigations



Part I – Clinical Application Developments
Femoroplasty

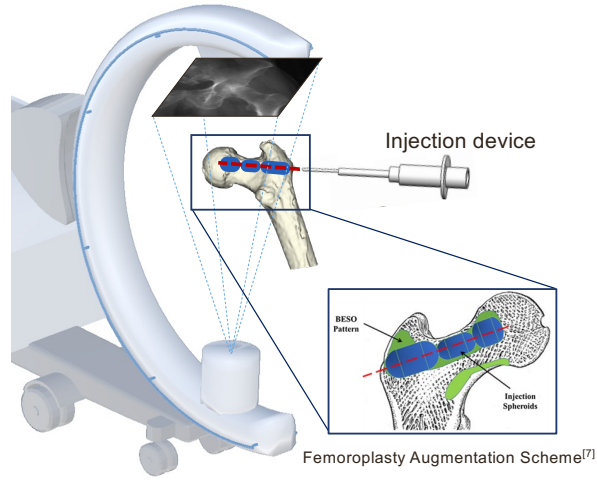
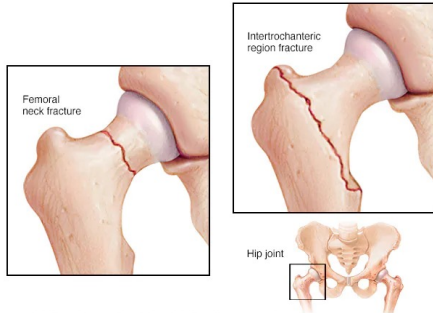


Clinical Background



Femoroplasty

- A preventive therapeutic procedure proposed for patients with osteoporosis
- Inject bone cement to an osteoporotic femur to reduce the risk of fracture



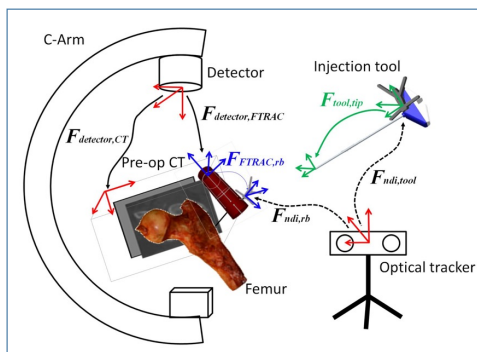
[7] Farvardin, A., Basafa, E., Bakhtiarijrad, M., & Armand, M. (2019). Significance of preoperative planning for prophylactic augmentation of osteoporotic hip: A computational modeling study. *Journal of biomechanics*, 94, 75-81.



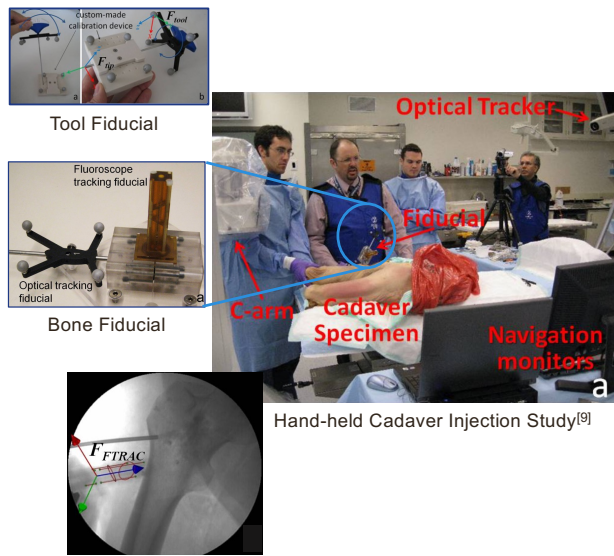
Previous Efforts: Hand-held Injection



Fiducial-based Navigation



Fiducial-based Femoroplasty System Configuration^{[8][9]}



[8] Otake, Y., Armand, M., Sadowsky, O., Armiger, R. S., Kutzer, M. D., Mears, S. C., ... & Taylor, R. H. (2010, February). An image-guided femoroplasty system: development and initial cadaver studies. In *Medical Imaging 2010: Visualization, Image-Guided Procedures, and Modeling* (Vol. 7625, p. 76250P). International Society for Optics and Photonics.

[9] Otake, Y., Armand, M., Armiger, R. S., Kutzer, M. D., Basafa, E., Kazanzides, P., & Taylor, R. H. (2011). Intraoperative image-based multiview 2D/3D registration for image-guided orthopaedic surgery: incorporation of fiducial-based C-arm tracking and GPU-acceleration. *IEEE transactions on medical imaging*, 31(4), 948-962.



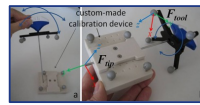
Previous Efforts: Hand-held Injection

Fiducial-based Navigation

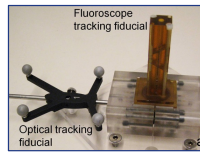
Limitations:

- Bone pin fiducial introduces additional incision to the patient
- Hand-held drilling is not stable
- X-ray field-of-view is limited to capture all fiducials

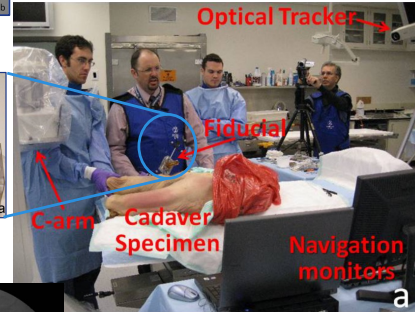
Fiducial-based Femoroplasty System Configuration^[8,9]



Tool Fiducial



Bone Fiducial



Hand-held Cadaver Injection Study^[9]



X-ray Example

[8] Otake, Y., Armand, M., Sadowsky, O., Armiger, R. S., Kutzer, M. D., Mears, S. C., ... & Taylor, R. H. (2010, February). An image-guided femoroplasty system: development and initial cadaver studies. In *Medical Imaging 2010: Visualization, Image-Guided Procedures, and Modeling* (Vol. 7625, p. 76250P). International Society for Optics and Photonics.
 [9] Otake, Y., Armand, M., Armiger, R. S., Kutzer, M. D., Basafa, E., Kazanzides, P., & Taylor, R. H. (2011). Intraoperative image-based multiview 2D/3D registration for image-guided orthopaedic surgery: incorporation of fiducial-based C-arm tracking and GPU-acceleration. *IEEE transactions on medical imaging*, 31(4), 948-962.

Robot-Assisted Femoroplasty

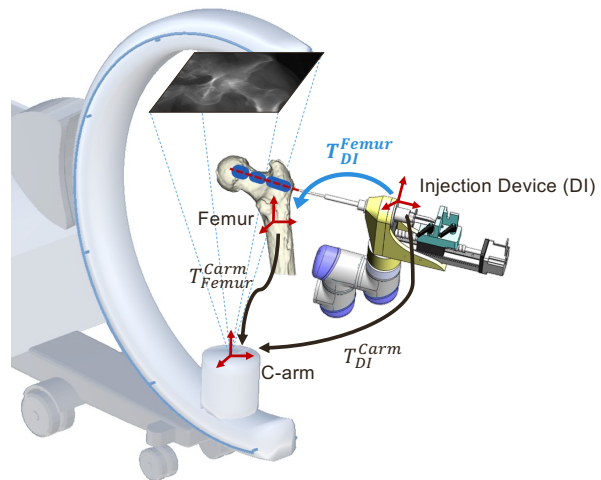
Proposed Objectives

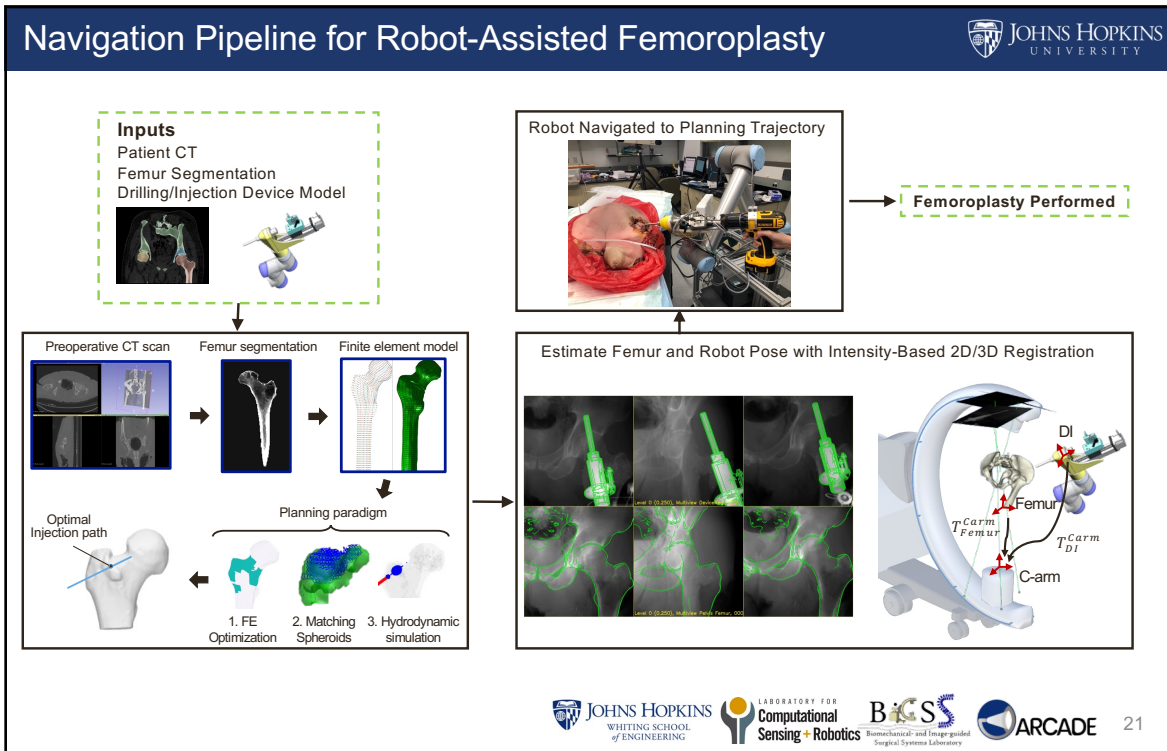
Robotic Drilling/Injection

- UR-10 as a steady positioning robot arm

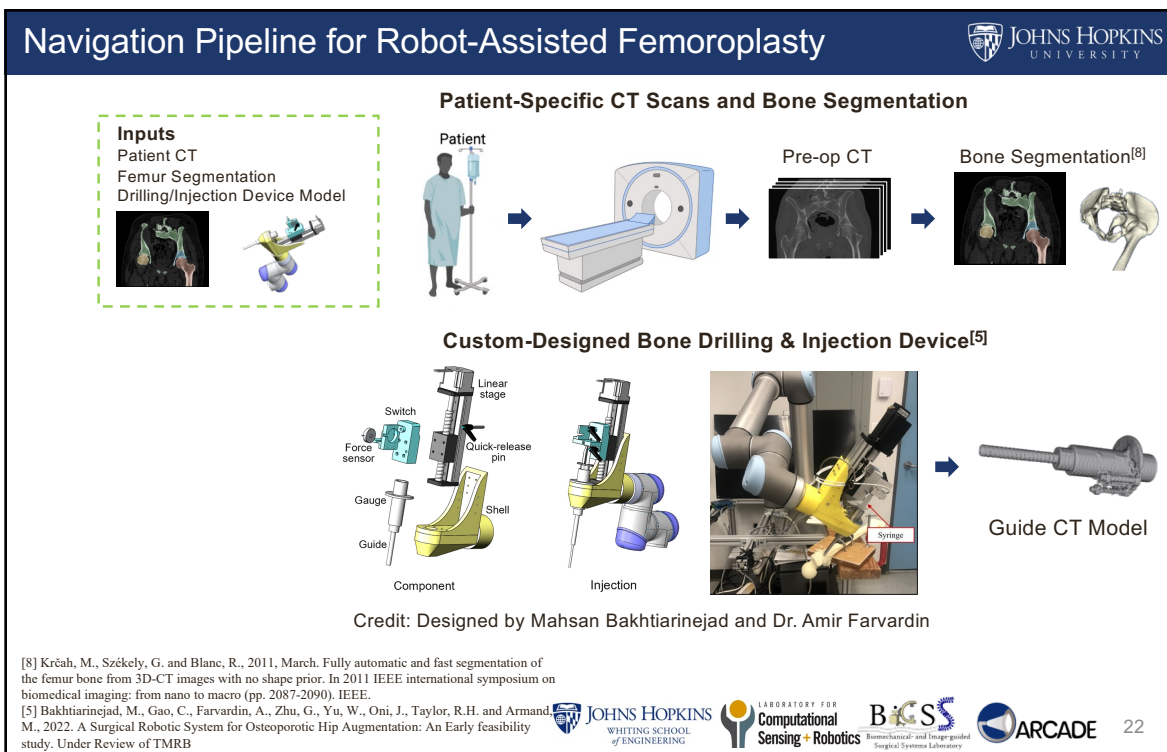
Fiducial-free Navigation

- Use purely C-arm X-ray images to estimate the critical T_{DI}^{Femur}





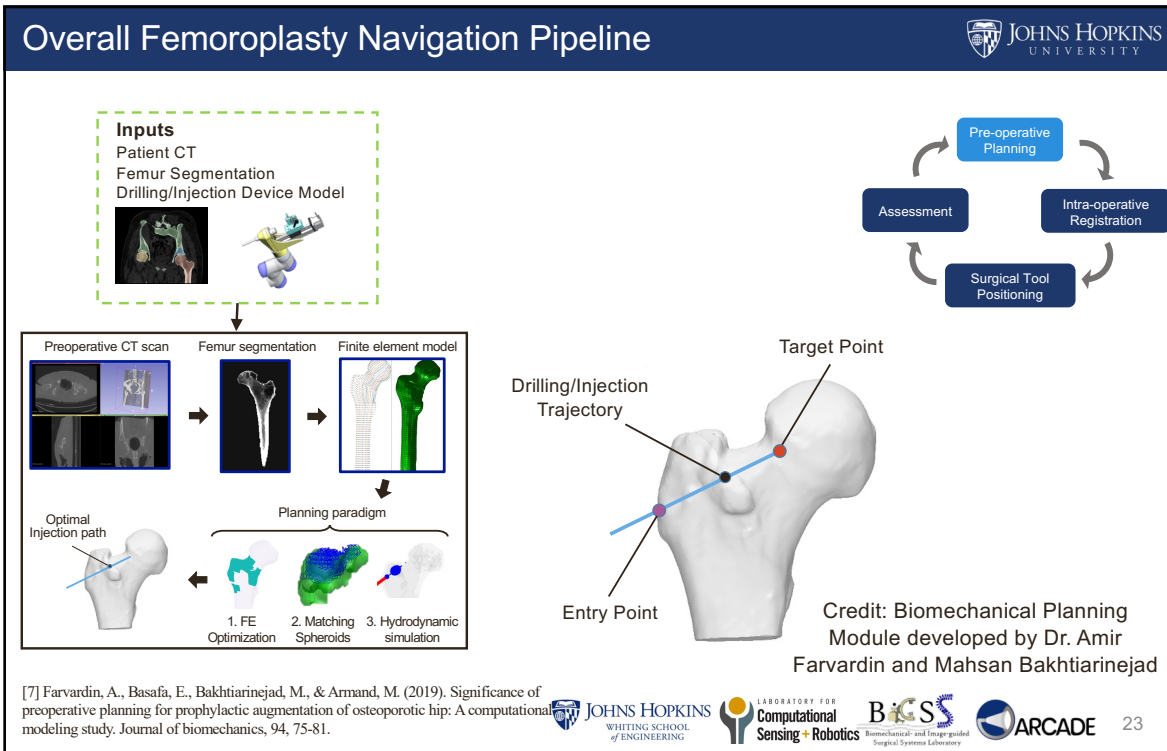
21



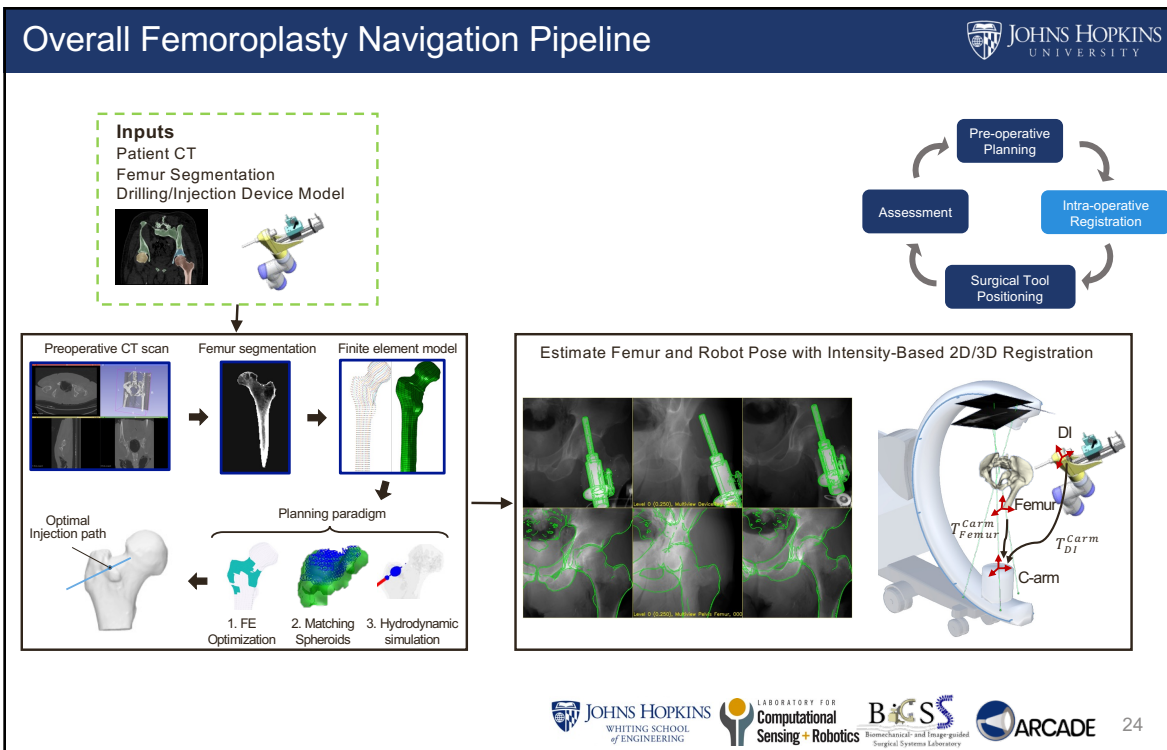
22

[8] Krčah, M., Székely, G. and Blanc, R., 2011, March. Fully automatic and fast segmentation of the femur bone from 3D-CT images with no shape prior. In 2011 IEEE international symposium on biomedical imaging: from nano to macro (pp. 2087-2090). IEEE.

[5] Bakhtiarinejad, M., Gao, C., Farvardin, A., Zhu, G., Yu, W., Oni, J., Taylor, R.H. and Armand, M., 2022. A Surgical Robotic System for Osteoporotic Hip Augmentation: An Early feasibility study. Under Review of TMRB



23

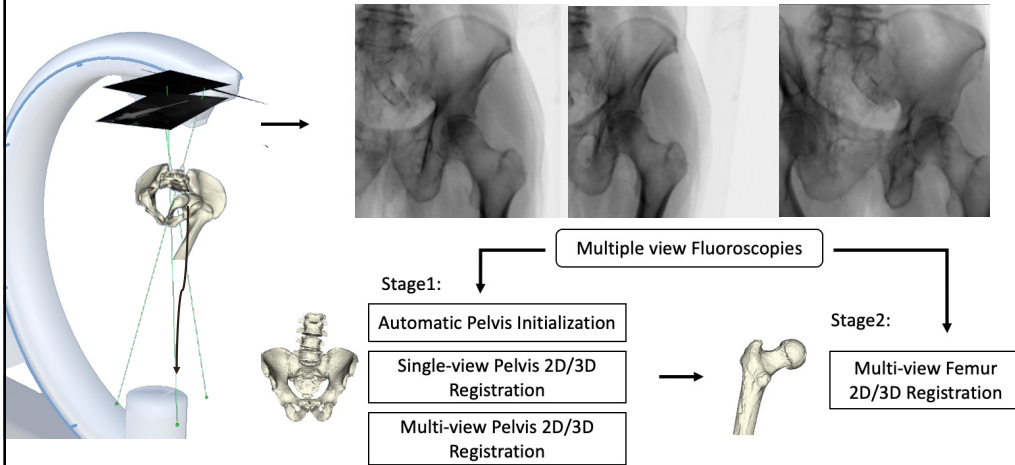


24

Registration Methods



Femur Registration Pipeline



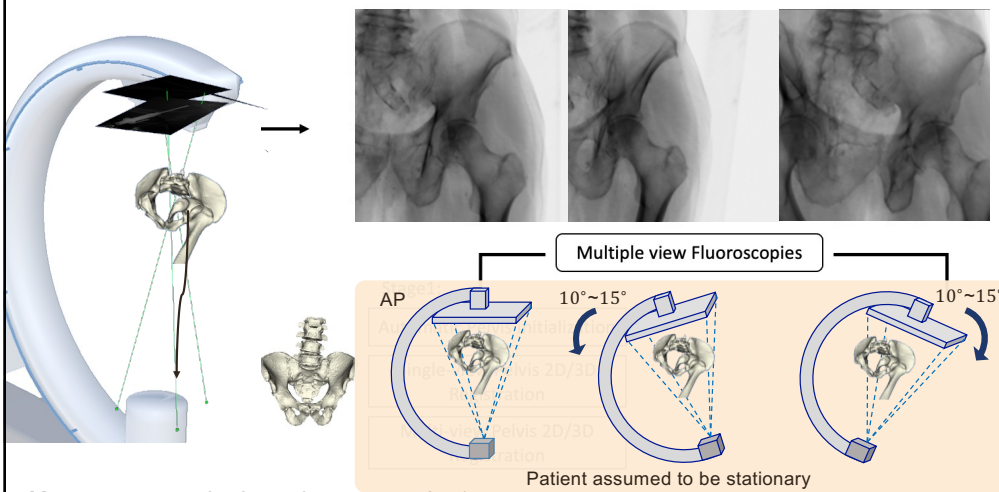
[9] Gao, C., Grupp, R. B., Unberath, M., Taylor, R. H., & Armand, M. (2020, March). Fiducial-free 2D/3D registration of the proximal femur for robot-assisted femoroplasty. In Medical Imaging 2020: Image-Guided Procedures, Robotic Interventions, and Modeling (Vol. 11315, p. 113151C). International Society for Optics and Photonics.



Registration Methods



Multi-view Data Acquisition



[9] Gao, C., Grupp, R. B., Unberath, M., Taylor, R. H., & Armand, M. (2020, March). Fiducial-free 2D/3D registration of the proximal femur for robot-assisted femoroplasty. In Medical Imaging 2020: Image-Guided Procedures, Robotic Interventions, and Modeling (Vol. 11315, p. 113151C). International Society for Optics and Photonics.



Registration Methods



Pelvis Registration

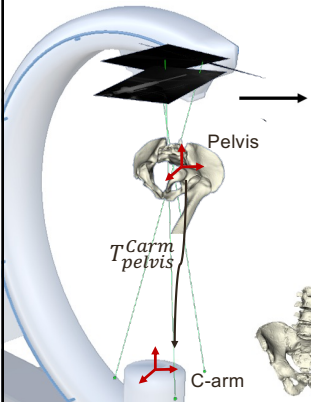
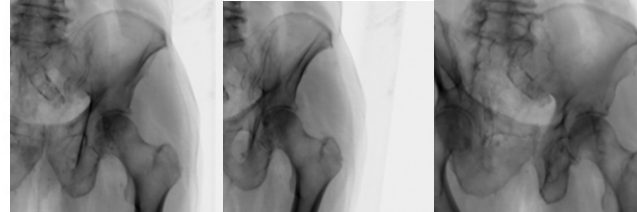


Diagram illustrating the registration setup. A C-arm is positioned around a pelvis. The transformation matrix T_{pelvis}^{Carm} is shown. The pelvis is labeled, and the C-arm is also labeled.

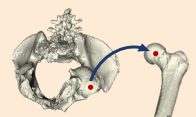


Three X-ray views of a pelvis, showing different perspectives.

Multiple views

Reason:

- Pelvis registration is more accurate than femur [11], because it is bigger and has more textures
- Pelvis registration estimates multi-view C-arm geometry
- Initialize and regularize femur registration



Stage1:

- Automatic Pelvis Initialization
- Single-view Pelvis 2D/3D Registration
- Multi-view Pelvis 2D/3D Registration

[11] Grupp, R.B., Hegeman, R.A., Murphy, R.J., Alexander, C.P., Otake, Y., McArthur, B.A., Armand, M. and Taylor, R.H., 2019. Pose estimation of periacetabular osteotomy fragments with intraoperative X-ray navigation. IEEE Transactions on Biomedical Engineering, 67(2), pp.441-452.



27

Registration Methods



Pelvis Registration

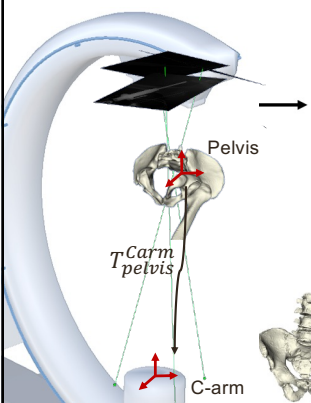
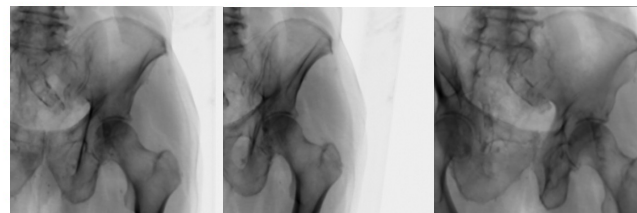


Diagram illustrating the registration setup. A C-arm is positioned around a pelvis. The transformation matrix T_{pelvis}^{Carm} is shown. The pelvis is labeled, and the C-arm is also labeled.



Three X-ray views of a pelvis, showing different perspectives.

Multiple view Fluoroscopies

Automatic Initialization

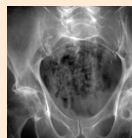
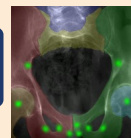
Stage2:

Concurrent Segmentation and Localization[1]

Solve a PnP problem using corresponding landmarks

Stage1:

- Automatic Pelvis Initialization
- Single-view Pelvis 2D/3D Registration
- Multi-view Pelvis 2D/3D Registration

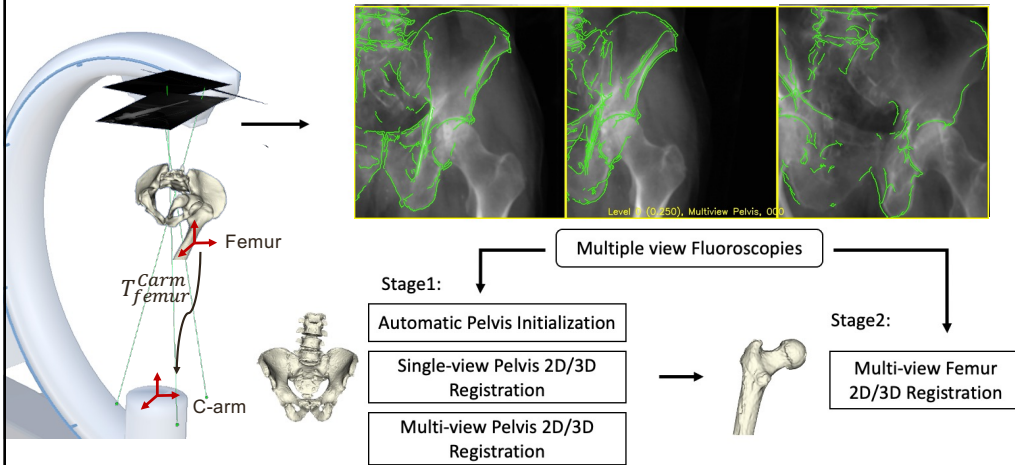
[10] Grupp, R.B., Unberath, M., Gao, C., Hegeman, R.A., Murphy, R.J., Alexander, C.P., Otake, Y., McArthur, B.A., Armand, M. and Taylor, R.H., 2020. Automatic annotation of hip anatomy in fluoroscopy for robust and efficient 2D/3D registration. International journal of computer assisted radiology and surgery, 15(5), pp.759-769.



28

Registration Methods

Femur Registration

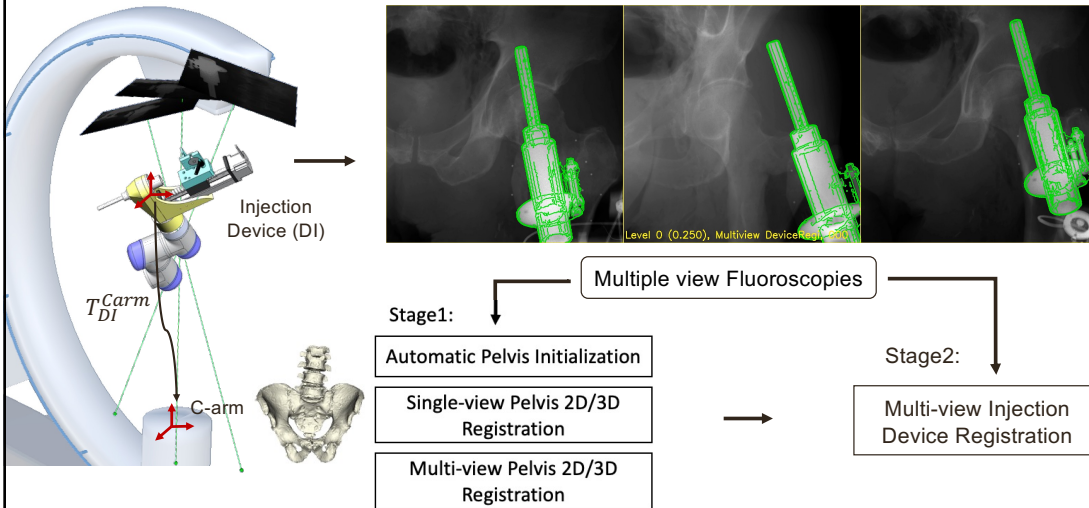


[9] Gao, C., Grupp, R. B., Unberath, M., Taylor, R. H., & Armand, M. (2020, March). Fiducial-free 2D/3D registration of the proximal femur for robot-assisted femoroplasty. In Medical Imaging 2020: Image-Guided Procedures, Robotic Interventions, and Modeling (Vol. 11315, p. 113151C). International Society for Optics and Photonics.

29

Registration Methods

Injection Device Registration



[12] Gao, C., Farvardin, A., Grupp, R.B., Bakhtiarnejad, M., Ma, L., Thies, M., Unberath, M., Taylor, R.H. and Armand, M., 2020. Fiducial-free 2D/3D registration for robot-assisted femoroplasty. IEEE transactions on medical robotics and bionics, 2(3), pp.437-446.

30

Registration Simulation Study

Simulated 1,000 Registrations with Randomized Geometries

Guide Tip
Entry Point

Table: Simulation Error

	mean	median
Entry Point (mm)	1.70 ± 0.94	1.64
Guide Tip (mm)	0.93 ± 0.81	0.74
Relative (mm)	1.26 ± 0.74	1.15
Femur Path (°)	0.63 ± 0.21	0.62
Guide Path (°)	0.17 ± 0.19	0.14

Femur entry point relative to Guide tip

$$Dist_{12} = \| (p_{carm}^{FEPgt} - p_{carm}^{FEPest}) - (p_{carm}^{IDTgt} - p_{carm}^{IDTest}) \|_2$$

Pelvis Pose Error

Femur Pose Error

Injection Device Pose Error

Joint Histogram of Translation and Rotation Errors

[12] Gao, C., Farvardin, A., Grupp, R.B., Bakhtiarnejad, M., Ma, L., Thies, M., Unberath, M., Taylor, R.H. and Armand, M., 2020. Fiducial-free 2D/3D registration for robot-assisted femoroplasty. IEEE transactions on medical robotics and bionics, 2(3), pp.437-446.

31

31

Femoroplasty Registration Cadaver Experiment

Cadaveric Experiment Setup

Ground truth pose obtained using metallic BB annotations, solving a PnP problem.

C-arm
specimen
Injection Device

BB
BB

Credit: BB injection performed by Dr. Liuhong Ma

[12] Gao, C., Farvardin, A., Grupp, R.B., Bakhtiarnejad, M., Ma, L., Thies, M., Unberath, M., Taylor, R.H. and Armand, M., 2020. Fiducial-free 2D/3D registration for robot-assisted femoroplasty. IEEE transactions on medical robotics and bionics, 2(3), pp.437-446.

32

32

Femoroplasty Registration Cadaver Experiment



Cadaveric Experiment Result

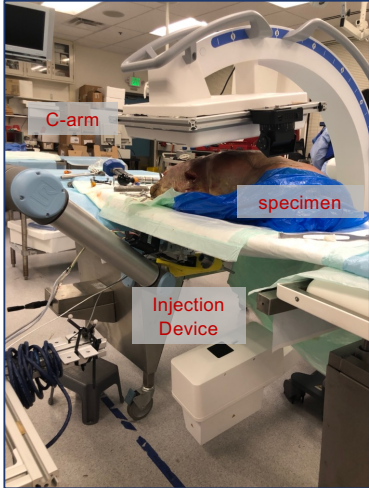


Table: Positional Registration Error of Six Individual Trials

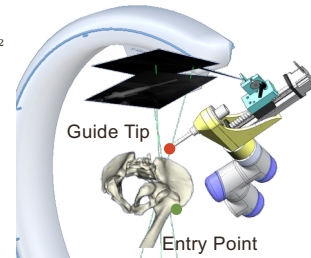
mm	Trial1	Trial2	Trial3	Trial4	Trial5	Trial6
Entry Point	1.34	2.44	2.41	1.99	3.67	4.38
Device Tip	3.17	0.84	1.48	2.93	1.79	0.83
Relative	1.98	2.88	3.44	1.32	1.94	4.28

Femur entry point relative to Guide tip

$$Dist_{12} = \| (P_{carm}^{FEPgt} - P_{carm}^{FEPst}) - (P_{carm}^{DTgt} - P_{carm}^{DTst}) \|_2$$

Mean Relative Error: **2.64 ± 1.10 mm**

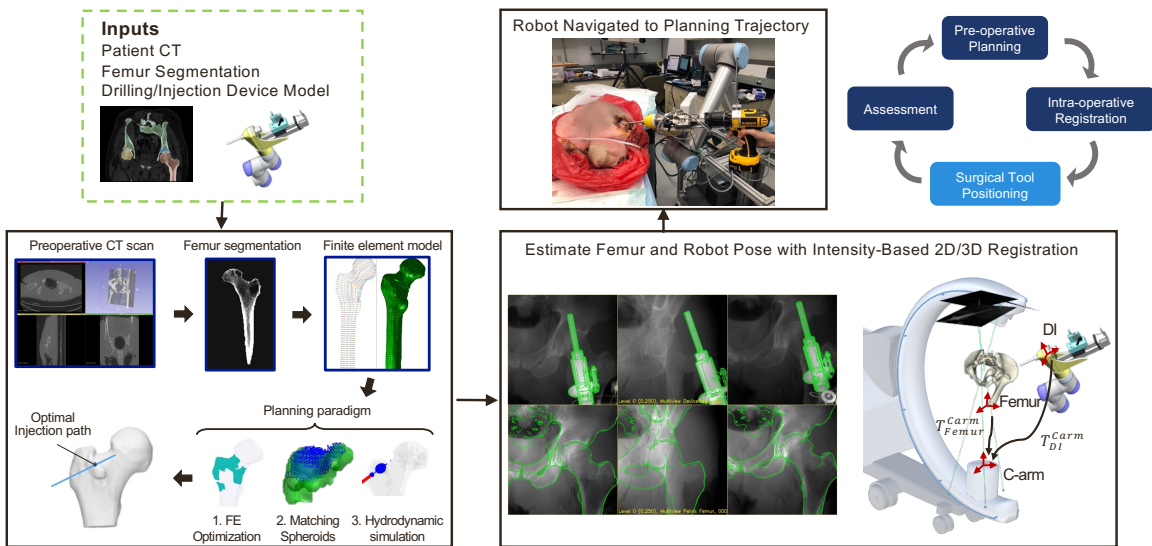
Clinically Acceptable Error: 2 - 3 mm



[12] Gao, C., Farvardin, A., Grupp, R.B., Bakhtiarnejad, M., Ma, L., Thies, M., Unberath, M., Taylor, R.H. and Armand, M., 2020. Fiducial-free 2D/3D registration for robot-assisted femoroplasty. IEEE transactions on medical robotics and bionics, 2(3), pp.437-446.



Overall Femoroplasty Navigation Pipeline



System Calibration



Hand-eye Calibration

- Solve an axxb problem

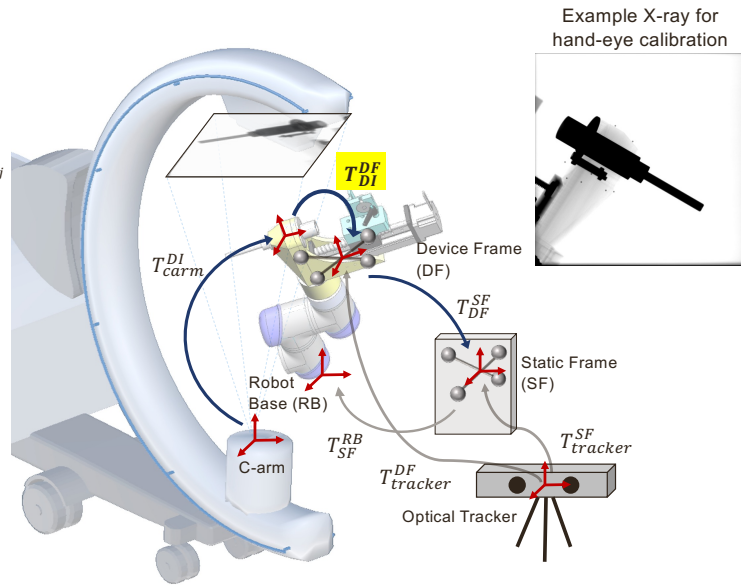
$$(T_{carm}^{DI})_i \cdot T_{DI}^{DF} \cdot (T_{DF}^{SF})_i = (T_{carm}^{DI})_j \cdot T_{DI}^{DF} \cdot (T_{DF}^{SF})_j$$

$$(T_{carm}^{DI})_j^{-1} (T_{carm}^{DI})_i \cdot T_{DI}^{DF} = T_{DI}^{DF} \cdot (T_{DF}^{SF})_j (T_{DF}^{SF})_i^{-1}$$

$$AX = XB$$

Note:
The tracker is used for closed-loop control, because the UR forward kinematic accuracy is insufficient for this task.

Credit: Closed-loop control module developed by Henry Phalen



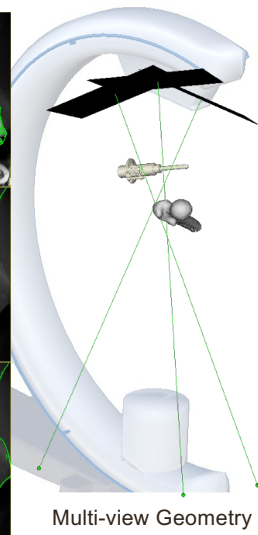
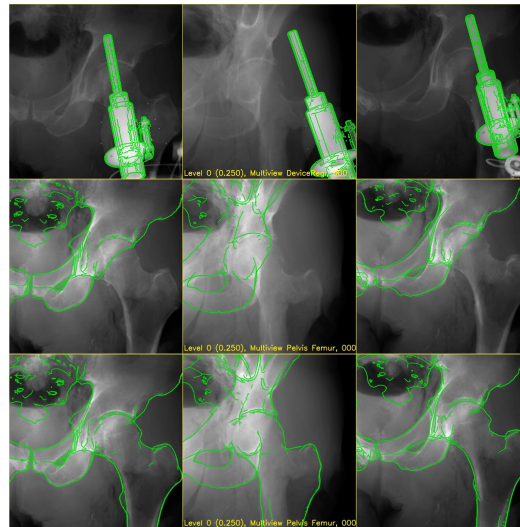
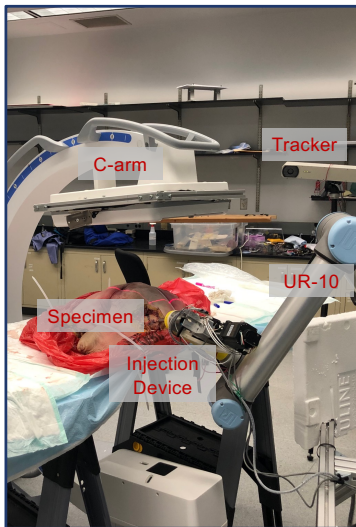
[5] Bakhtiarinejad, M., Gao, C., Farvardin, A., Zhu, G., Yu, W., Oni, J., Taylor, R.H. and Armand, M., 2022. A Surgical Robotic System for Osteoporotic Hip Augmentation: An Early feasibility study. Under Review of TMRB



Femoroplasty System Integration Cadaver Experiment



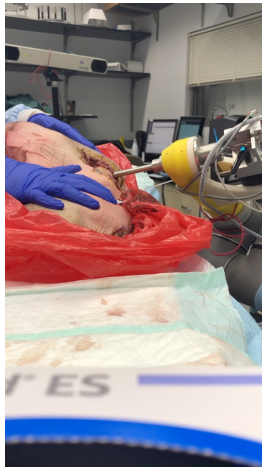
Cadaver Experiment Setup and Registration Visualizations



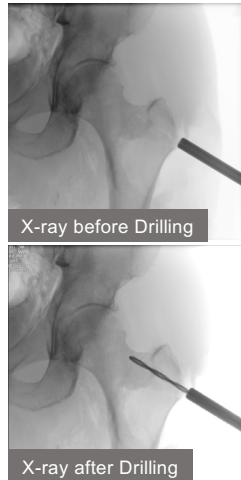
[5] Bakhtiarinejad, M., Gao, C., Farvardin, A., Zhu, G., Yu, W., Oni, J., Taylor, R.H. and Armand, M., 2022. A Surgical Robotic System for Osteoporotic Hip Augmentation: An Early feasibility study. Under Review of TMRB



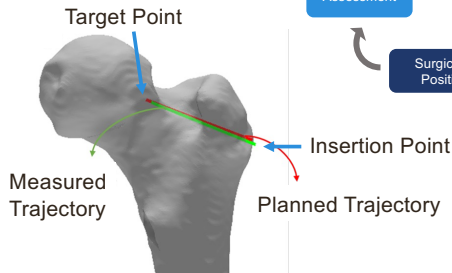
Cadaveric Drilling and Results



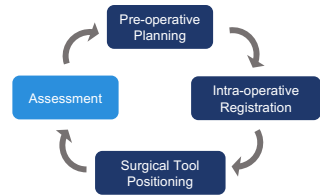
Drilling after the guide is positioned



Post-op CT Analysis



Target point error: 2.64 mm
 Insertion point error: 3.28 mm
 Orientation error: 2.30 degrees



[5] Bakhtiarnejad, M., Gao, C., Farvardin, A., Zhu, G., Yu, W., Oni, J., Taylor, R.H. and Armand, M., 2022. A Surgical Robotic System for Osteoporotic Hip Augmentation: An Early feasibility study. Under Review of TMRB

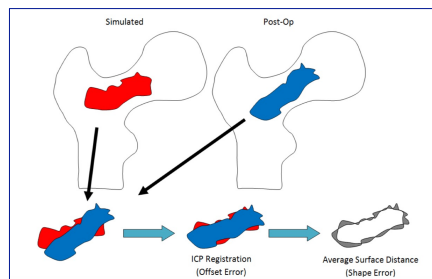
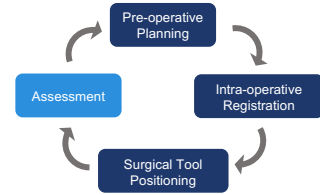


Clinical Evaluation



Yield load estimation with biomechanical simulation:

- **33% increase** of yield load with the measured trajectory error
- Previous biomechanical studies show **positive augmentation effects** when distance error $\sim 8\text{mm}$, rotation error $\sim 5^\circ$ [13]



Credit: Yield load estimation performed by Mahsan Bakhtiarnejad

[5] Bakhtiarnejad, M., Gao, C., Farvardin, A., Zhu, G., Yu, W., Oni, J., Taylor, R.H. and Armand, M., 2022. A Surgical Robotic System for Osteoporotic Hip Augmentation: An Early feasibility study. Under Review of TMRB

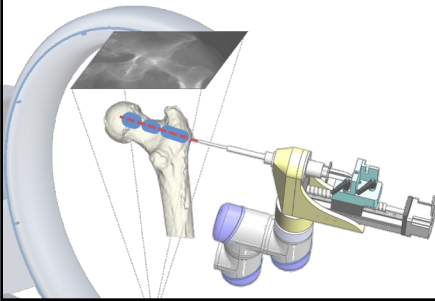
[13] Basafa, Ehsan. Computer-Assisted Femoral Augmentation For Osteoporotic Fracture Prevention. Diss. Johns Hopkins University, 2013.



Conclusion and Contributions



- An automatic, intensity-based 2D/3D registration method for pose estimation of the femur
- A fiducial-free navigation pipeline for robot-assisted femoroplasty
- Evaluated the navigation methods with simulation and cadaver experiments. The results meet clinical requirements, and suggest feasibility to be used for related orthopedic applications



39

39

Acknowledgment



Dr. Robert Grupp: Developed 2D/3D registration software infrastructure - xreg, contributed to femur registration algorithm design

Mrs. Mahsan Bakhtiarinejad and Dr. Amir Farvardin: Designed the injection unit, developed biomechanical analysis pipeline, contributed to cadaver experiments and analysis

Mr. Henry Phalen: Developed the robot closed-loop control module

Dr. Lihong Ma and Ms. Mareike Thies: Helped with cadaver experiments

Related Publications/Manuscripts:

- **Gao, C.,** Farvardin, A., Grupp, R.B., Bakhtiarinejad, M., Ma, L., Thies, M., Unberath, M., Taylor, R.H. and Armand, M., 2020. Fiducial-free 2D/3D registration for robot-assisted femoroplasty. IEEE transactions on medical robotics and bionics, 2(3), pp.437-446.
- **Gao, C.,** Grupp, R. B., Unberath, M., Taylor, R. H., & Armand, M. (2020, March). Fiducial-free 2D/3D registration of the proximal femur for robot-assisted femoroplasty. In Medical Imaging 2020: Image-Guided Procedures, Robotic Interventions, and Modeling (Vol. 11315, p. 113151C). International Society for Optics and Photonics.
- Bakhtiarinejad, M., **Gao, C.,** Farvardin, A., Zhu, G., Yu, W., Oni, J., Taylor, R.H. and Armand, M., 2022. A Surgical Robotic System for Osteoporotic Hip Augmentation: An Early feasibility study. Under Review of TMRB



40

40

Part I – Clinical Application Developments

Lumbar Epidural Injections



41

Clinical Background



Pain Relief from Spine Epidural Injections

- Globally, between 60-80% of people are expected to experience lower back pain in lifetime
- 30 million epidural injections worldwide
- Effectiveness is highly variable (50-70% efficacy rates)
- Failed injections can result in catastrophic spinal cord or nerve root injuries, even paralysis



Example Spine Needle Injection^[13]

[13] <https://www.spineuniverse.com/treatments/pain-management/thoracic-epidural-injection>
 [14] <https://orthoinfo.aaos.org/en/treatment/spinal-injections/>

42

Clinical Background

Clinical Practice and Challenges

The clinician acquires several fluoroscopic images before and during the manual insertion of the needle

Lack of 3D needle position estimation with respect to the spine vertebrae



Clinician's needle injection under fluoroscopic guidance^[15]

[15] <https://www.vapainsc.com/treatments-and-procedures/lumbar-epidural-steroid-injections%E2%80%933-transforaminal.html>

Autonomous Robotic Spinal Needle Insertion

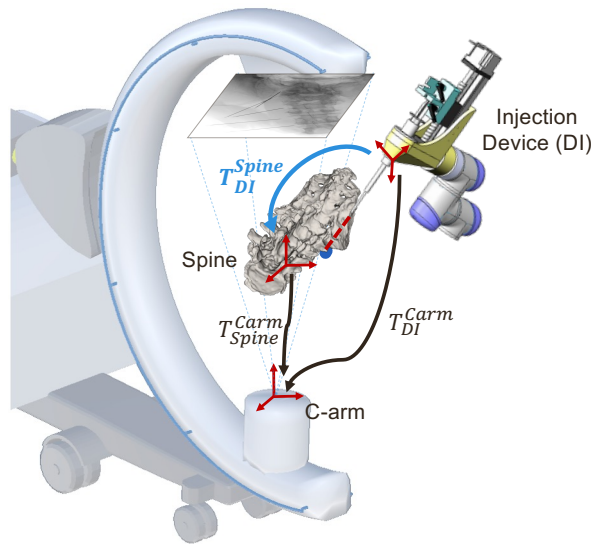
Proposed Objectives

Robotic Needle Injection

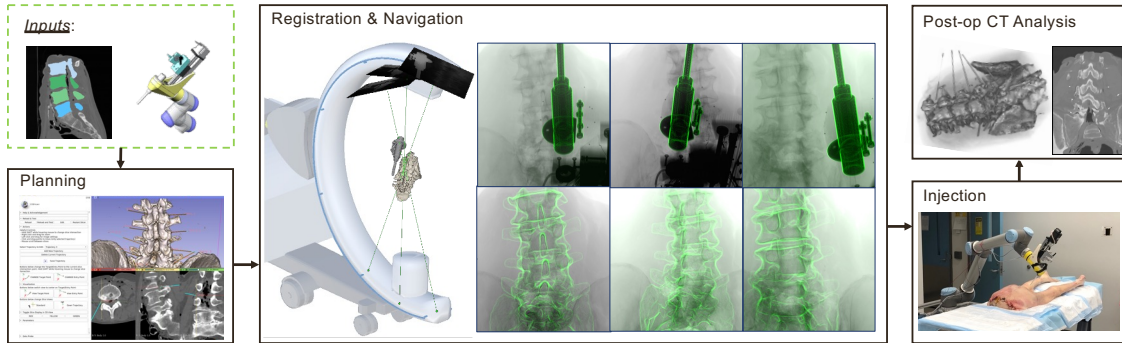
- Robotic End Effector delivers the needle

Fiducial-Free Navigation

- Use purely C-arm X-ray images to estimate the critical T_{DI}^{Spine}



Spine Injection Navigation Pipeline

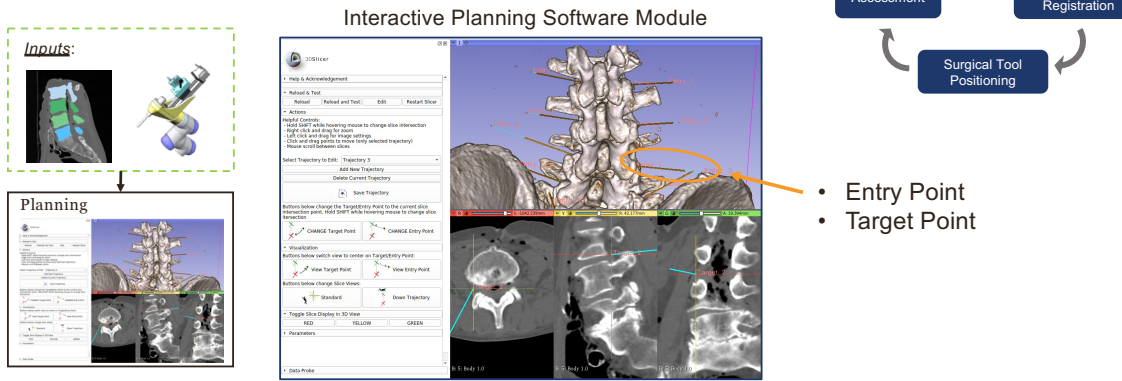


[15] Gao, C*, Phalen, H*, Maraglit, A, Ma, J., Ku, P, Unberath, M., Taylor, R., Jain, A. and Armand, M. 2022 Fluoroscopy-Guided Robotic System for Transforaminal Lumbar Epidural Injections. Under Review of TMRB
 * indicates joint first co-authors



45

Overall Spine Injection Navigation Pipeline



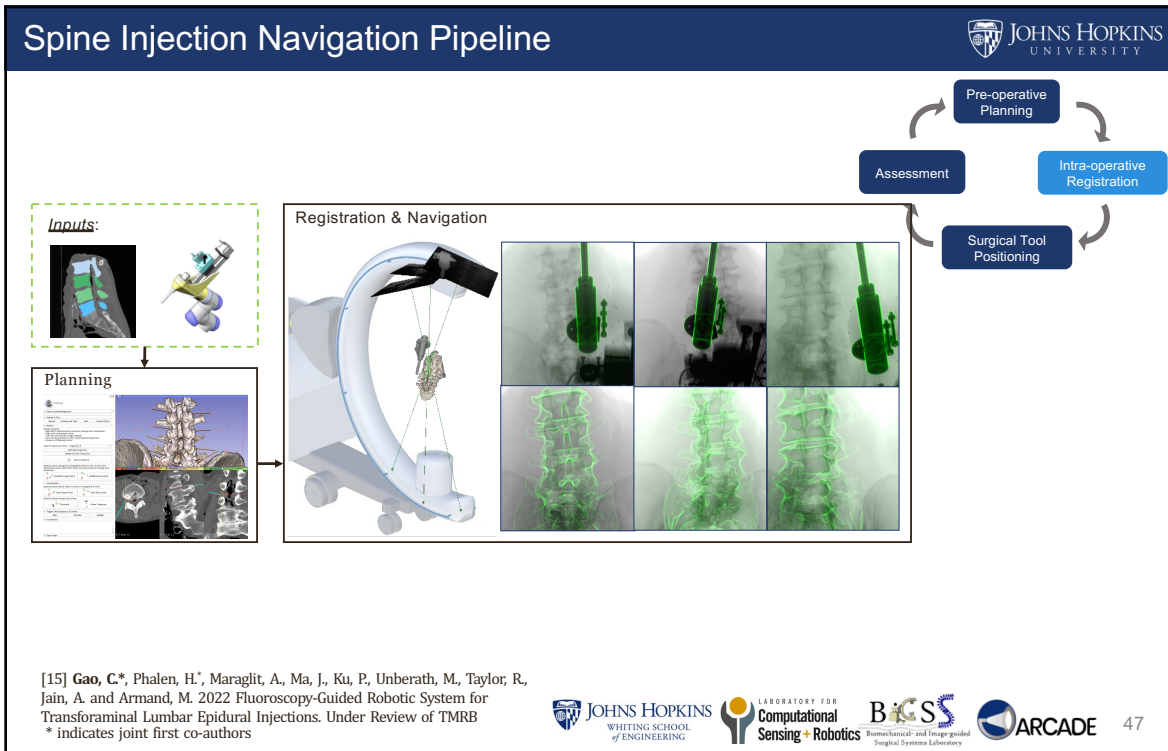
- Entry Point
- Target Point

Credit: Interactive Planning Module developed by Henry Phalen

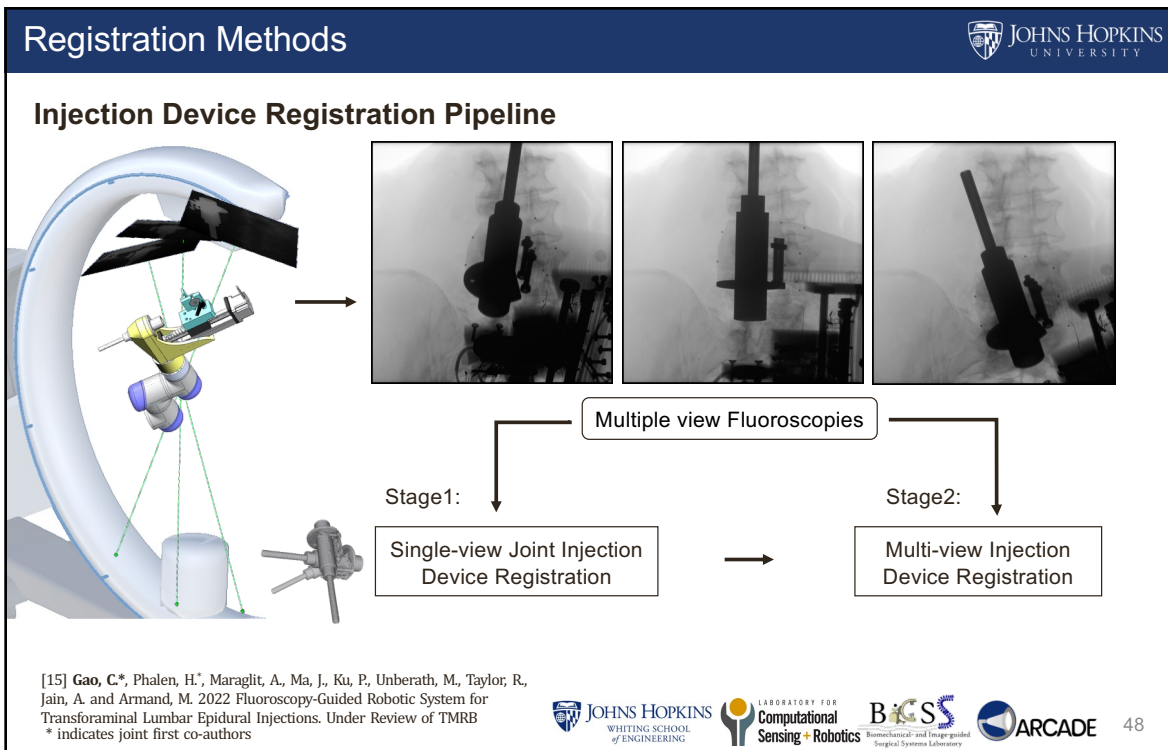
[15] Gao, C*, Phalen, H*, Maraglit, A, Ma, J., Ku, P, Unberath, M., Taylor, R., Jain, A. and Armand, M. 2022 Fluoroscopy-Guided Robotic System for Transforaminal Lumbar Epidural Injections. Under Review of TMRB
 * indicates joint first co-authors



46



47



48

Registration Methods



Joint Injection Device Registration

Stage 1: Single-view Joint Injection Device Registration

Multiple

Joint registration using robot kinematics information

- Balance single-view registration ambiguity

C-arm is fixed, robot moves to multiple configurations

[15] Gao, C*, Phalen, H*, Maraglit, A, Ma, J., Ku, P, Unberath, M., Taylor, R., Jain, A. and Armand, M. 2022 Fluoroscopy-Guided Robotic System for Transforaminal Lumbar Epidural Injections. Under Review of TMRB
 * indicates joint first co-authors



Registration Methods



Joint Injection Device Registration

Stage 1: Single-view Joint Injection Device Registration

Multiple

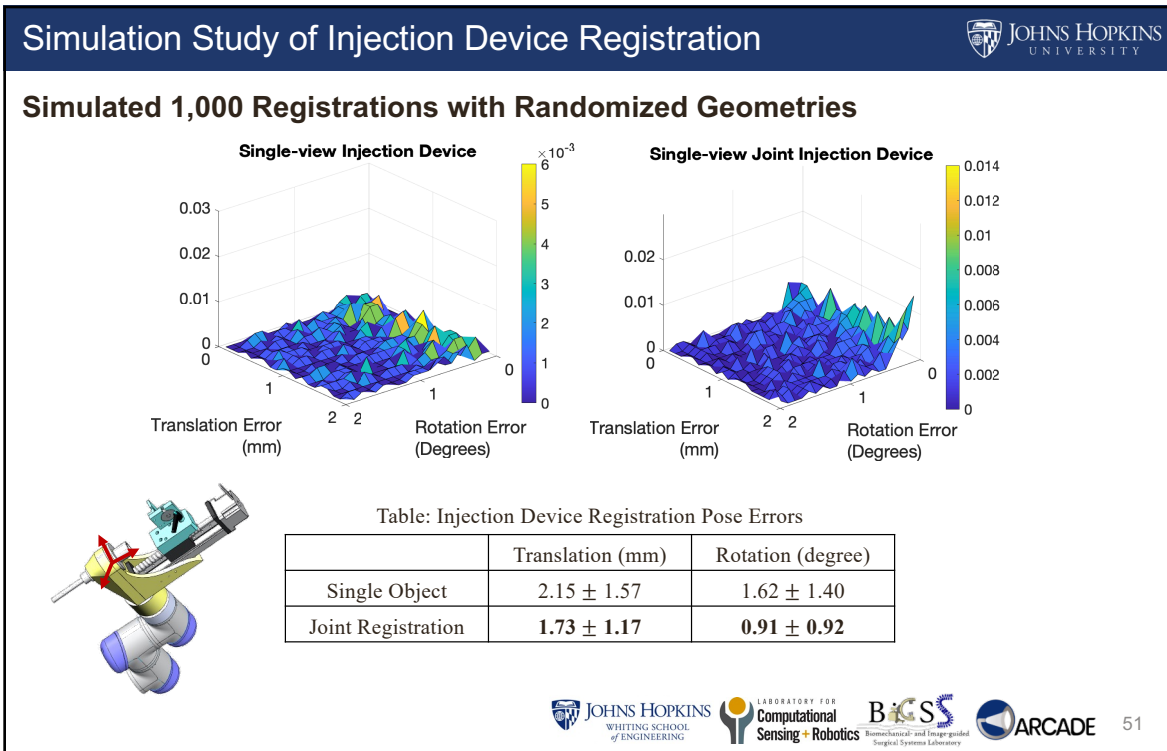
Joint registration using robot kinematics information

- Balance single-view registration ambiguity

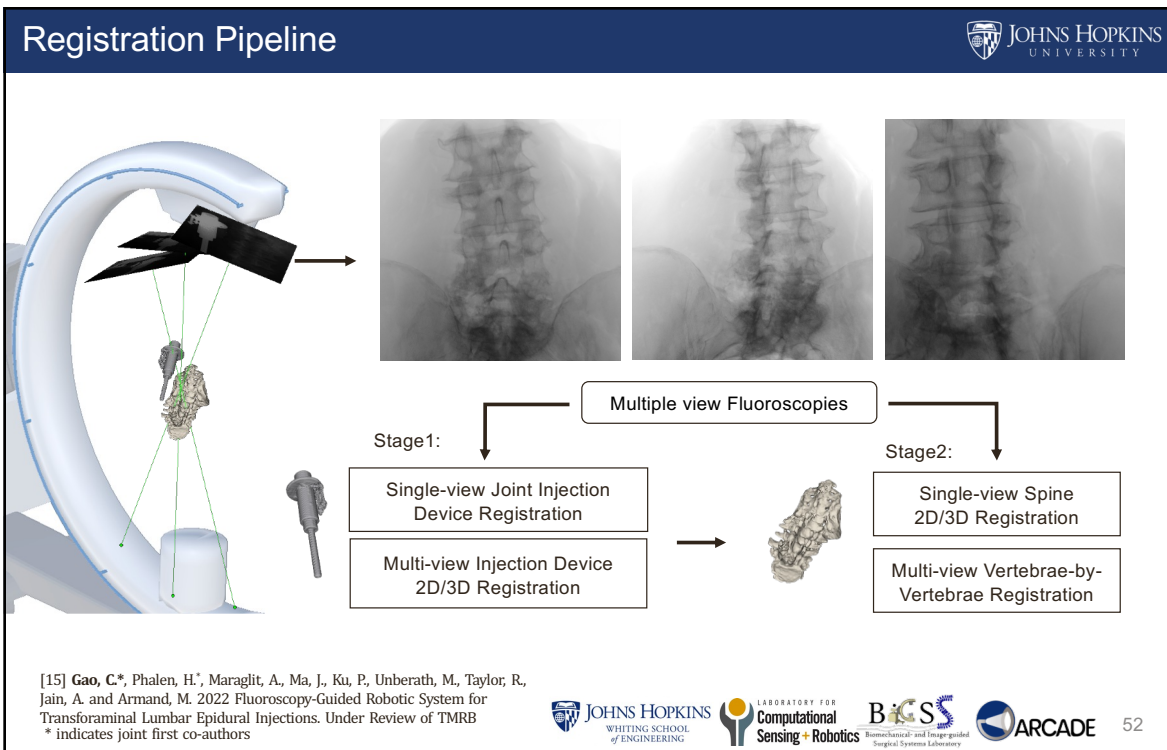
C-arm is fixed, robot moves to multiple configurations

[15] Gao, C*, Phalen, H*, Maraglit, A, Ma, J., Ku, P, Unberath, M., Taylor, R., Jain, A. and Armand, M. 2022 Fluoroscopy-Guided Robotic System for Transforaminal Lumbar Epidural Injections. Under Review of TMRB
 * indicates joint first co-authors



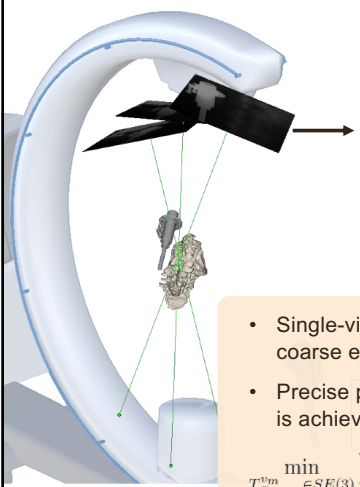


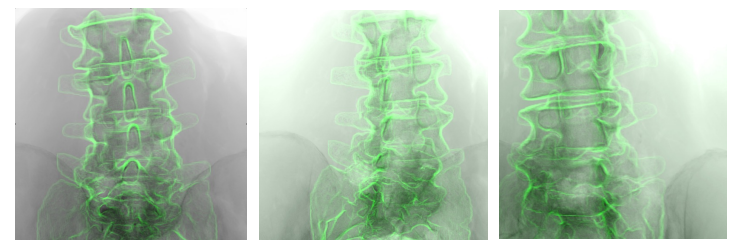
51



52

Registration Pipeline





Multiple view Fluoroscopies

- Single-view rigid spine registration provides a coarse estimation
- Precise pose estimation of individual vertebra is achieved by multi-component optimization


$$\min_{T_{Carm_0}^{m_0} \in SE(3)} \sum_{k=1}^K \mathcal{S} \left(I_k^S, \mathcal{P} \left(\sum_{m=1}^M V_m; T_{Carm_0}^{m_0}, T_{Carm_k}^{m_k} \right) \right)$$

Loop every vertebra

Stage2:

- Single-view Spine 2D/3D Registration
- Multi-view Vertebrae-by-Vertebrae Registration

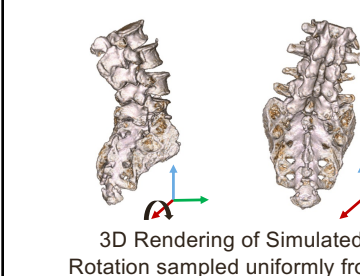
[15] Gao, C*, Phalen, H*, Maraglit, A., Ma, J., Ku, P., Unberath, M., Taylor, R., Jain, A. and Armand, M. 2022 Fluoroscopy-Guided Robotic System for Transforaminal Lumbar Epidural Injections. Under Review of TMRB
 * indicates joint first co-authors

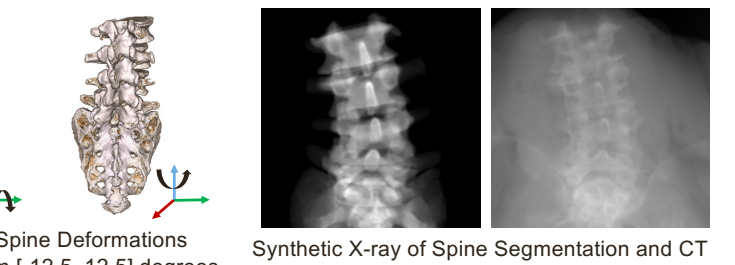


53

53

Spine Registration Simulation Study






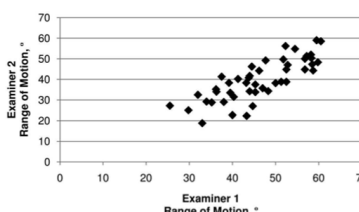
Synthetic X-ray of Spine Segmentation and CT

Simulate Spine Deformation using CT Segmentations

3D Rendering of Simulated Spine Deformations
 Rotation sampled uniformly from [-12.5, 12.5] degrees


Spine Range of Motion^[16]





40 - 60 degrees for normal adult

[16] Johnson, K.D., Kim, K.M., Yu, B.K., Saliba, S.A. and Grindstaff, T.L., 2012. Reliability of thoracic spine rotation range-of-motion measurements in healthy adults. Journal of athletic training, 47(1), pp.52-60.



54

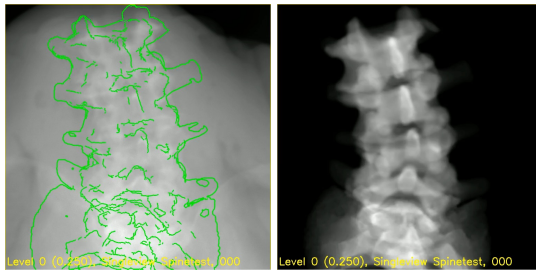
54

Spine Registration Simulation Study

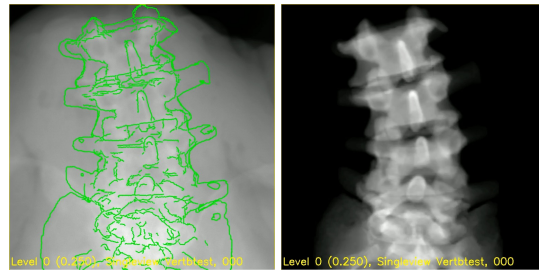


Single-view C-arm Geometry

Rigid Spine Registration



Vertebrae-by-Vertebrae Registration



[15] Gao, C*, Phalen, H*, Maraglit, A, Ma, J., Ku, P., Unberath, M., Taylor, R., Jain, A. and Armand, M. 2022 Fluoroscopy-Guided Robotic System for Transforaminal Lumbar Epidural Injections. Under Review of TMRB
* indicates joint first co-authors



55

55

Spine Registration Simulation Study

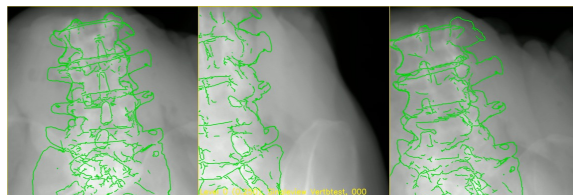


Multi-view C-arm Geometry

Rigid Spine Registration



Vertebrae-by-Vertebrae Registration

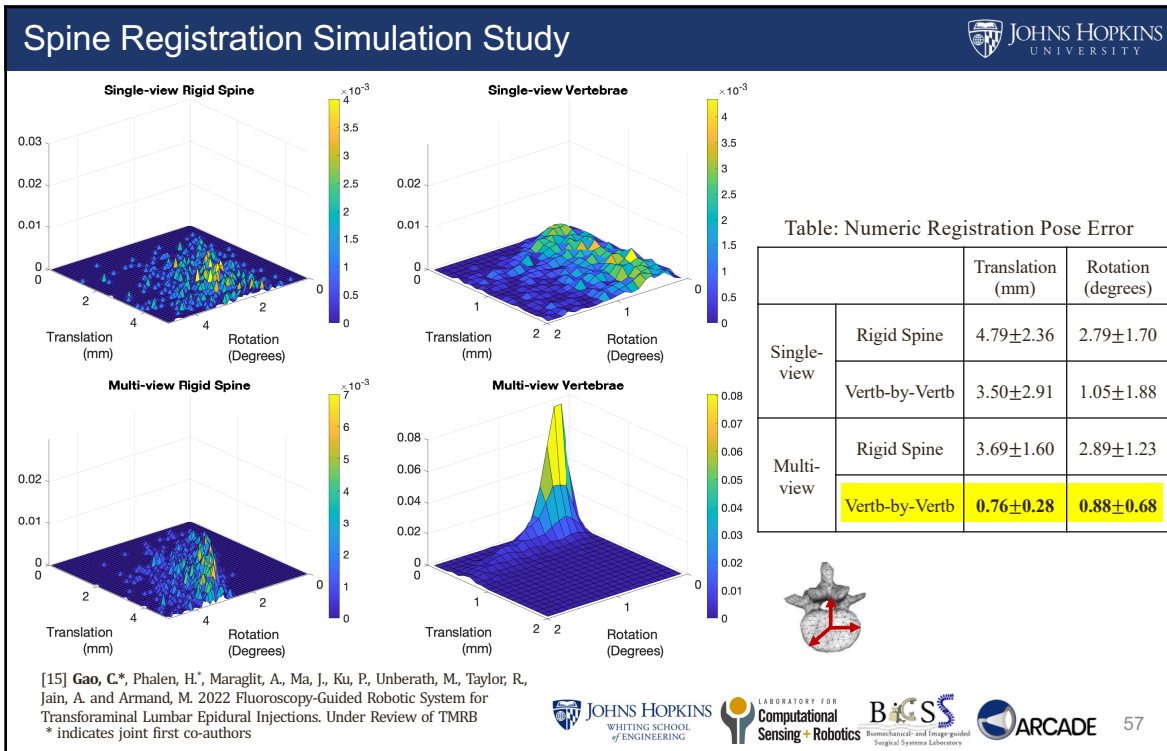


[15] Gao, C*, Phalen, H*, Maraglit, A, Ma, J., Ku, P., Unberath, M., Taylor, R., Jain, A. and Armand, M. 2022 Fluoroscopy-Guided Robotic System for Transforaminal Lumbar Epidural Injections. Under Review of TMRB
* indicates joint first co-authors

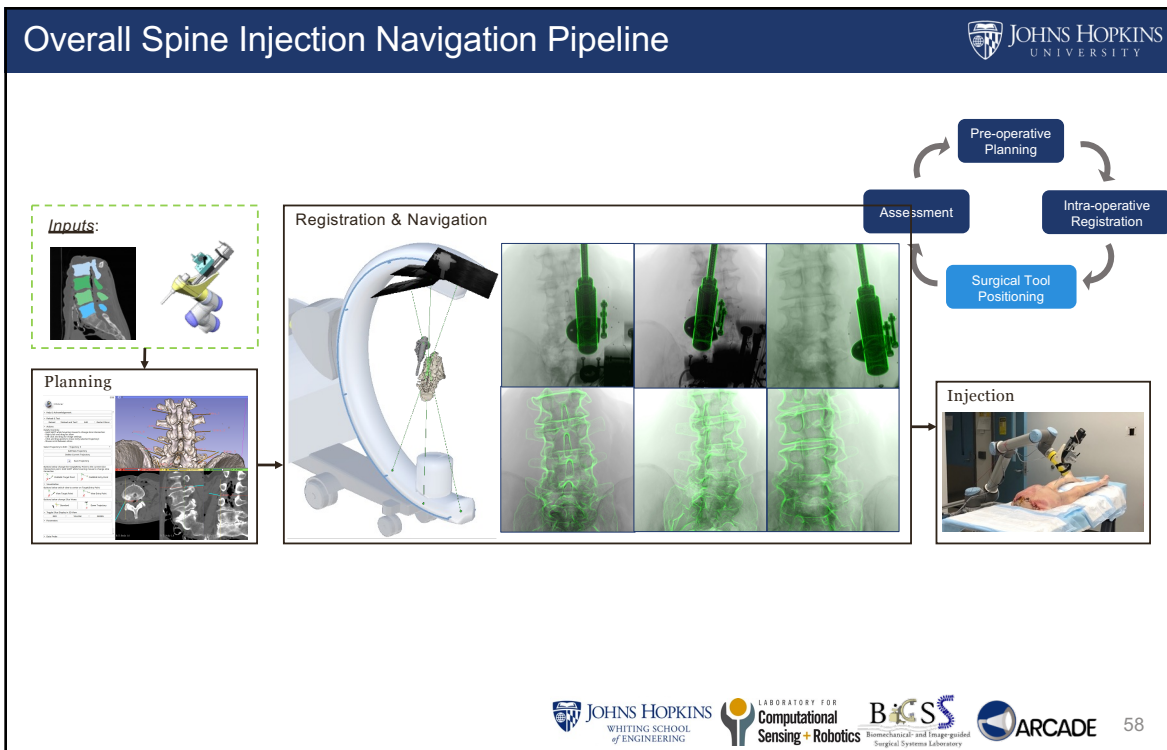


56

56



57



58

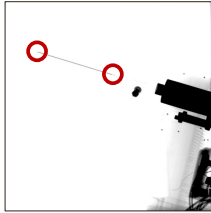
System Setup



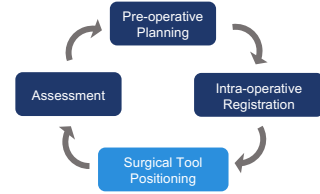
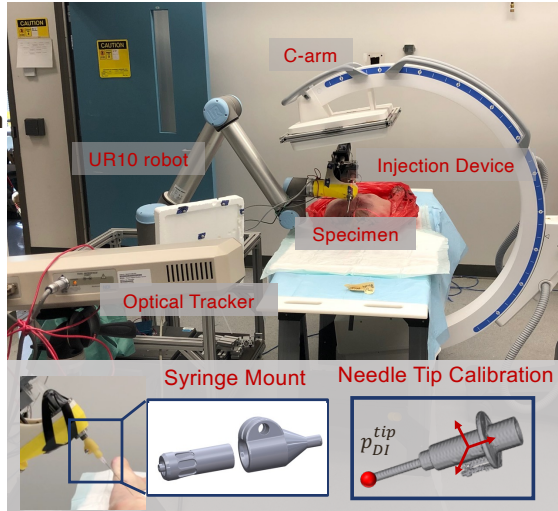
Hand-eye Calibration

- Introduced before

Needle Tip Calibration



- Triangulate the needle tip point in the injection model frame using 6-7 X-ray images



Credit: The Syringe mount is designed by Justin Ma

[15] Gao, C*, Phalen, H*, Maraglit, A, Ma, J., Ku, P., Unberath, M., Taylor, R., Jain, A. and Armand, M. 2022 Fluoroscopy-Guided Robotic System for Transforaminal Lumbar Epidural Injections. Under Review of TMRB
 * indicates joint first co-authors



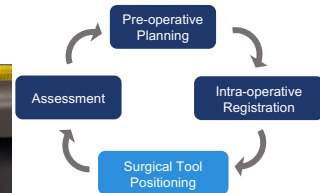
Robotic Spine Needle Injection Cadaver Study



Performed 10 Robotic Needle Injections



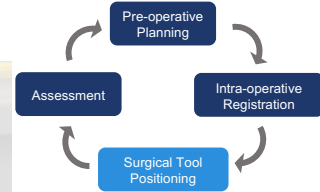
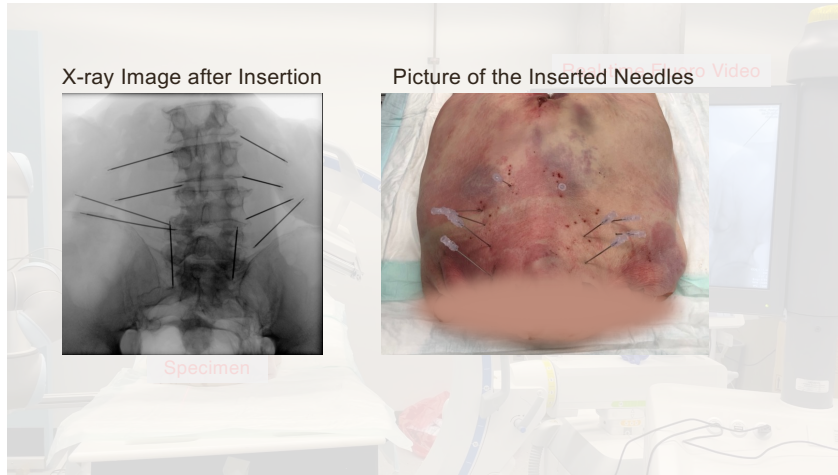
Robot Injection Experiment Video



Robotic Spine Needle Injection Cadaver Study



Performed 10 Robotic Needle Injections



Robot Injection Experiment Video



61

Experienced Clinician Manual Injection



Performed 10 Needle Injections using the same Plannings



62

Spine Injection Results



Post-op Analysis

- Took post-op CT scans with inserted needles
- 3D/3D Registration between pre-op and post-op CT of each individual vertebra
- Annotated target/entry points for comparison

Table: Cadaveric Needle Injection Accuracy

ID	Needle Tip Error (mm)		Orientation Error (degrees)	
	Robot	Surgeon	Robot	Surgeon
1	3.13	9.46	5.13	5.77
2	6.13	11.35	1.85	8.30
3	7.02	6.17	2.40	13.20
4	7.14	12.29	4.60	6.98
5	4.36	6.88	2.06	9.28
6	1.54	8.46	1.56	8.61
7	5.14	3.36	2.63	7.05
8	8.01	7.02	5.52	20.88
9	1.57	5.28	2.95	13.46
10	6.85	5.56	7.37	5.51
Mean	5.09 ± 2.36	7.58 ± 2.80	3.61 ± 1.93	9.90 ± 4.73

[15] Gao, C*, Phalen, H*, Maraglit, A, Ma, J., Ku, P., Unberath, M., Taylor, R., Jain, A. and Armand, M. 2022 Fluoroscopy-Guided Robotic System for Transforaminal Lumbar Epidural Injections. Under Review of TMRB
 * indicates joint first co-authors

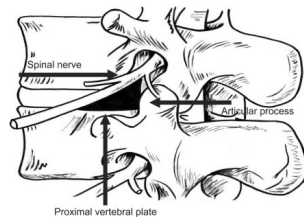


Clinical Evaluation

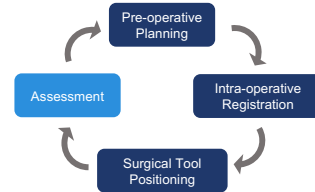
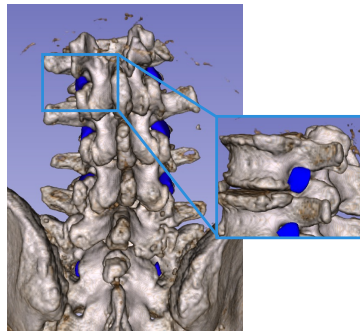


Triangle Safety Zone

- Injections through the safety triangle allow the steroid to be injected more effectively and safely
- All of our injections were within the triangle safety zones



Definition



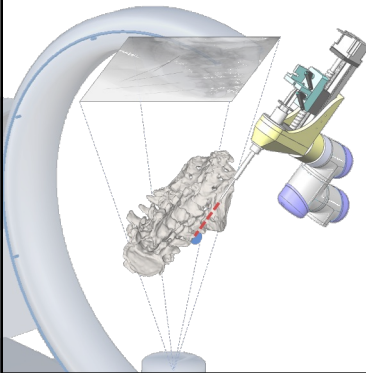
[15] Gao, C*, Phalen, H*, Maraglit, A, Ma, J., Ku, P., Unberath, M., Taylor, R., Jain, A. and Armand, M. 2022 Fluoroscopy-Guided Robotic System for Transforaminal Lumbar Epidural Injections. Under Review of TMRB
 * indicates joint first co-authors



Conclusion and Contributions



- An autonomous fluoroscopy-guided robotic spine needle injection system
- Present the superiority of multi-view, multi-component 2D/3D registration over single-view, single object 2D/3D registration with simulation experiments
- Present the improved performance using our robotic injections compared to clinician's manual injections in controlled cadaver experiments



65

65

Acknowledgment



Mr. Henry Phalen: Developed the interactive needle planning module, the robot closed-loop control module, contributed to system calibration and trouble shooting, jointly worked on both phantom and cadaver experiments, and post-op analysis

Mr. Adam Margalit: Built the spine testing phantom (not presented here), provided clinical guidance, coordination and equipment support, jointly worked on both phantom and cadaver experiments

Mr. Justin Ma: Developed the robot closed-loop control module

Mr. Ping-Cheng Ku: Helped annotate the triangle safety zone for post-op analysis

Dr. Akhil Chhatre and Dr. David Cohen: Performed manual needle injections

Related Publications/Manuscripts:

- **Gao, C.***, Phalen, H.*, Maraglit, A., Ma, J., Ku, P., Unberath, M., Taylor, R., Jain, A. and Armand, M. 2022 Fluoroscopy-Guided Robotic System for Transforaminal Lumbar Epidural Injections. Under Review of TMRB
- Margalit, A., Phalen, H., **Gao, C.**, Ma, J., Suresh, K.V., Jain, P., Farvardin, A., Taylor, R.H., Armand, M., Chhatre, A. and Jain, A., 2022. Autonomous Spinal Robotic System for Transforaminal Lumbar Epidural Injections: A Proof of Concept of Study. Global Spine Journal, p.21925682221096625.

* indicates joint first co-authors



66

66

Part I – Clinical Application Developments

Core Decompression of the Hip



67

Core Decompression of the Hip



Osteonecrosis

- A disease that results from loss of blood supply to the bone
- Usually progresses to femoral head collapse, and eventually **total hip arthroplasty**
- **Core Decompression** -- Reduce the pressure in the femoral head with osteonecrosis

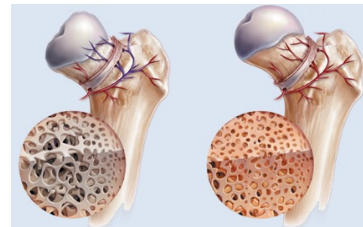
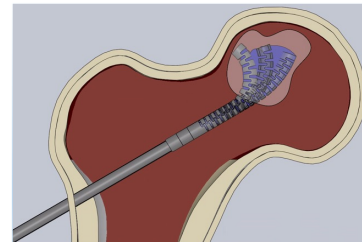


Illustration of Osteonecrosis^[17]

Less-invasive Surgical Procedure

- Access the lesion through the narrow femoral neck by drilling
- Remove and grafting the lesion



Concept of Curvature Drilling

[17] <https://www.spineorthocenter.com/services/orthopedic/joint-diseases/osteonecrosis/>



68

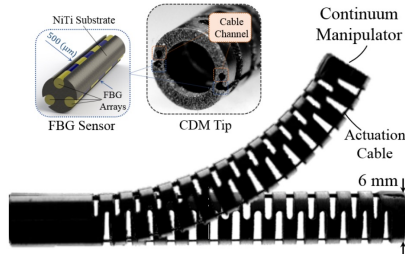
68

Continuum Manipulator

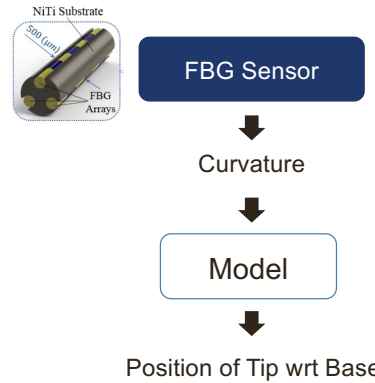


Custom-designed Continuum Manipulator with embedded Shape Sensing

- Accurate intraoperative pose and shape feedback during bone drilling is challenging



Continuum manipulator and FBG [18]



[18] Sefati, S., Hegeman, R., Alambeigi, F., Iordachita, I., & Armand, M. (2019, April). FBG-based position estimation of highly deformable continuum manipulators: Model-dependent vs. data-driven approaches. In 2019 International Symposium on Medical Robotics (ISMR) (pp. 1-6). IEEE

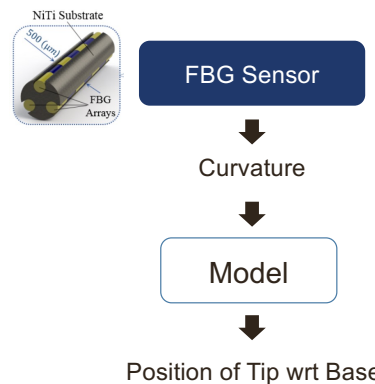
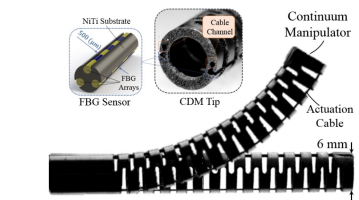


Continuum Manipulator



Challenges of FBG Shape Sensing

- Fiber Bragg Grating (FBG) sensing doesn't have enough sensing points, which might not be accurate
- Large errors when touching obstacles^[19]
- Internal sensing does not close the registration loop with respect to the bone



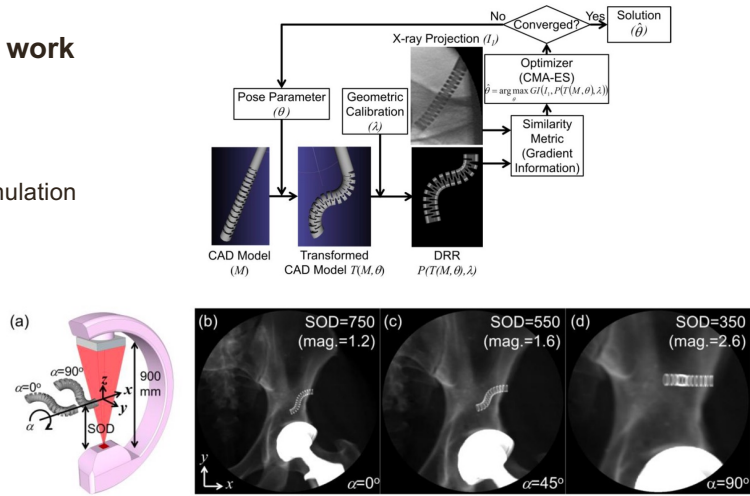
[19] Sefati, S., Hegeman, R., Alambeigi, F., Iordachita, I., & Armand, M. (2019, April). FBG-based position estimation of highly deformable continuum manipulators: Model-dependent vs. data-driven approaches. In 2019 International Symposium on Medical Robotics (ISMR) (pp. 1-6). IEEE



Previous Efforts

Limitations of Otake et al.'s work

- Manual initialization
- Only tested in simulation. The simulation was not yet realistic
- Not integrated/tested with the robot system

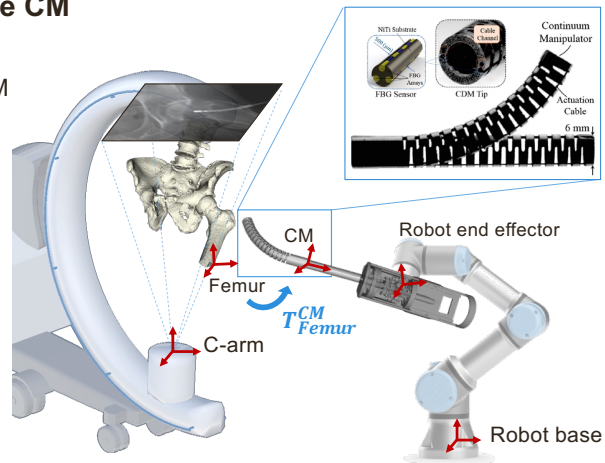


[21] Otake, Y., Murphy, R.J., Kutzer, M.D., Taylor, R.H. and Armand, M., 2014, March. Piecewise-rigid 2D-3D registration for pose estimation of snake-like manipulator using an intraoperative x-ray projection. In Medical Imaging 2014: Image-Guided Procedures, Robotic Interventions, and Modeling (Vol. 9036, pp. 185-190). SPIE.

Motivation

X-ray Image-based navigation of the CM

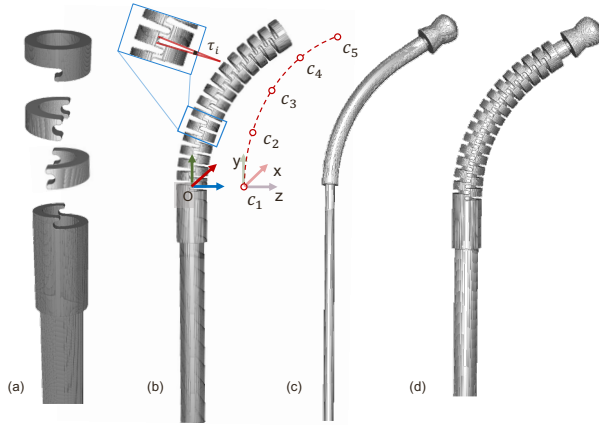
- Rigid Pose estimation of femur and the CM
- Flexible CM Shape estimation
- Robot relative to the bone anatomy, T_{Femur}^{CM}



CM Navigation Concept^[20]

[20] Gao, C., Phalen, H., Sefati, S., Ma, J., Taylor, R.H., Unberath, M. and Armand, M., 2021. Fluoroscopic navigation for a surgical robotic system including a continuum manipulator. IEEE Transactions on Biomedical Engineering, 69(1), pp.453-464.

CM Model and X-ray Simulation



CM 3D Model

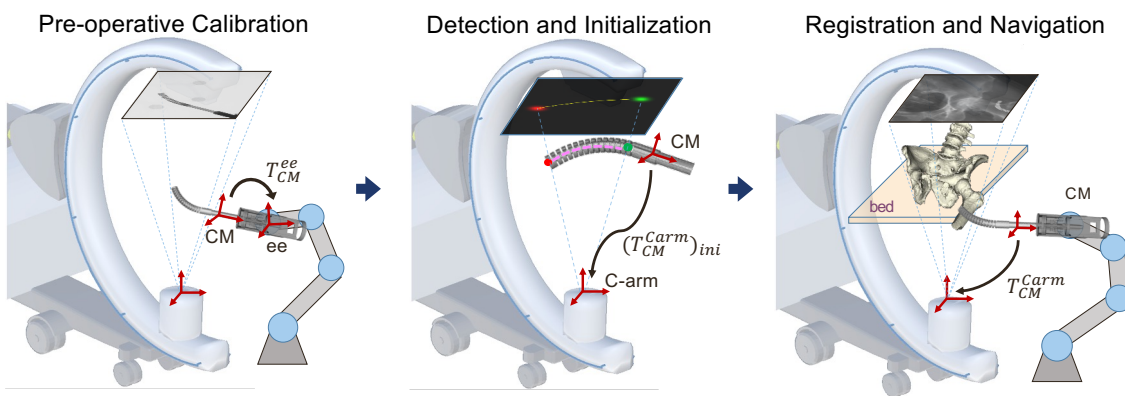


Example X-ray Simulation

[20] Gao, C., Phalen, H., Sefati, S., Ma, J., Taylor, R.H., Unberath, M. and Armand, M., 2021. Fluoroscopic navigation for a surgical robotic system including a continuum manipulator. IEEE Transactions on Biomedical Engineering, 69(1), pp.453-464.

73

CM Navigation Pipeline

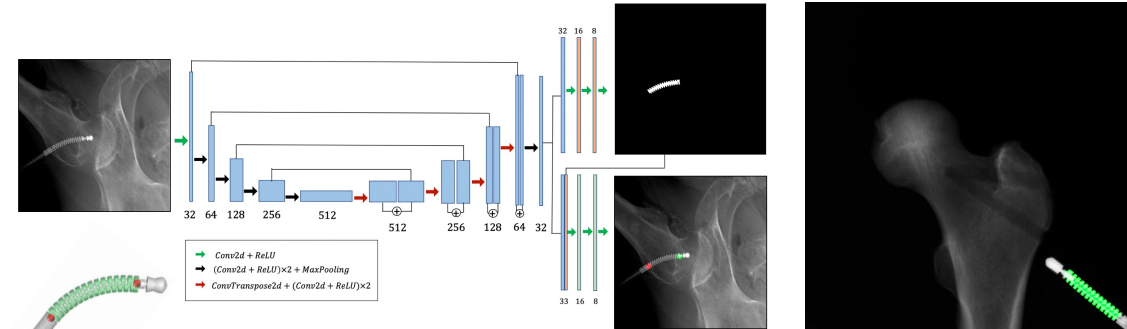


[20] Gao, C., Phalen, H., Sefati, S., Ma, J., Taylor, R.H., Unberath, M. and Armand, M., 2021. Fluoroscopic navigation for a surgical robotic system including a continuum manipulator. IEEE Transactions on Biomedical Engineering, 69(1), pp.453-464.

74

Learning-based CM Detection

Concurrent segmentation and landmark detection^[21]



Example real X-ray detection results

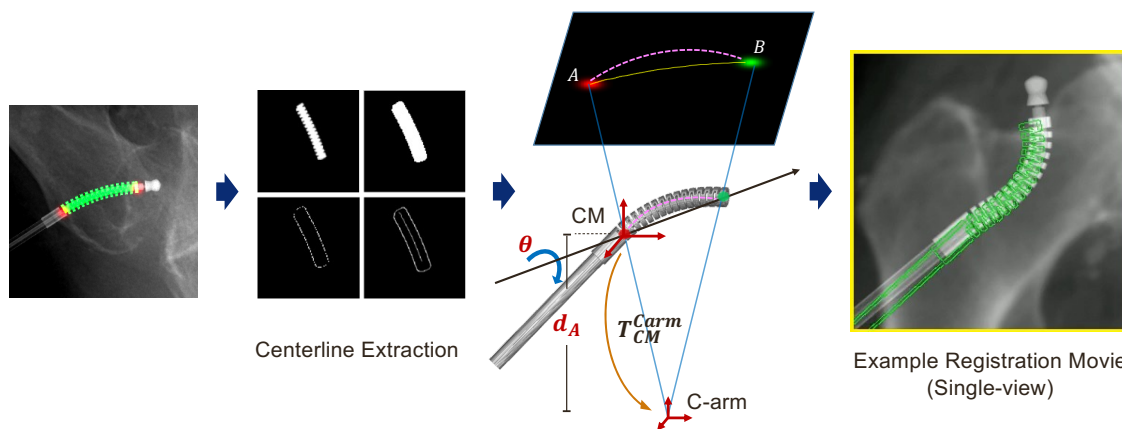
Table: CM Detection Accuracy

	Landmark Error (mm)	Segmentation DICE Score
Simulation	0.449 ± 0.525	0.993 ± 0.002
Real X-ray	2.62 ± 1.05	0.920 ± 0.068

[21] C. Gao*, M. Unberath*, R. Taylor, & M. Armand (2019). Localizing dexterous surgical tools in X-ray for image-based navigation. IPCAI 2019 Long Abstract

Single-view CM Registration

- Automatic initialization of CM registration
- The landmarks regularize the registration search space (reprojection penalty)

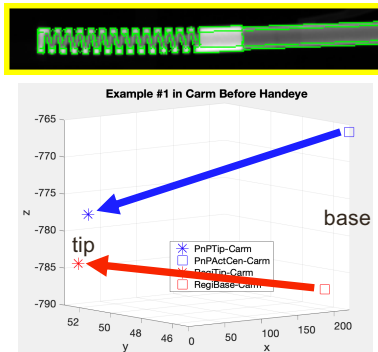


[20] Gao, C., Phalen, H., Sefati, S., Ma, J., Taylor, R.H., Unberath, M. and Armand, M., 2021. Fluoroscopic navigation for a surgical robotic system including a continuum manipulator. IEEE Transactions on Biomedical Engineering, 69(1), pp.453-464.

CM Registration

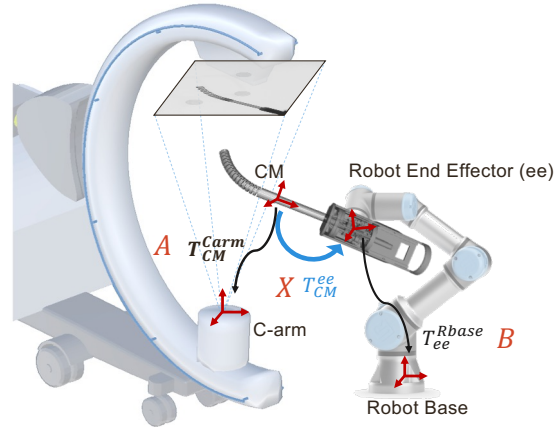
Severe Registration Ambiguity

- Single-view registration by itself has ambiguity
- The CM is small, symmetric and flexible



Affects the hand-eye calibration accuracy

- Solve an axyb problem

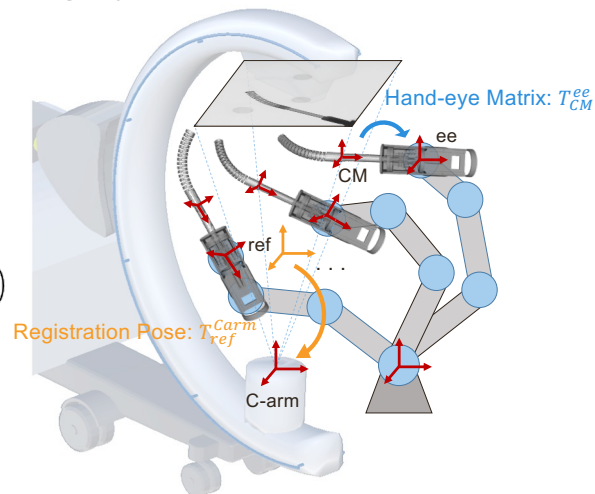


Joint CM Registration

Our Solution to Balance Registration Ambiguity

- Use robot kinematics to jointly register multiple CM configurations together
- A modified, image-based hand-eye calibration method

$$\min_{T_{ref}^{Carm}, T_{CM}^{ee} \in SE(3), \tau_i} \sum_{m=1}^M \mathcal{S} \left(I_k, \mathcal{P} \left(\sum_{j=1}^J V_j; T_{ref}^{Carm}, T_{CM}^{ee}, \tau_i \right) \right)$$



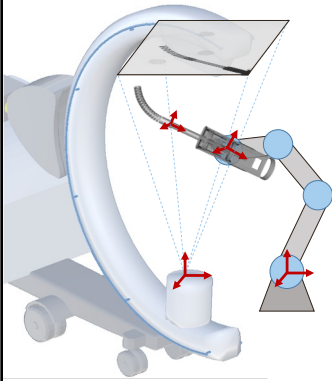
Joint CM Registration

[20] Gao, C., Phalen, H., Sefati, S., Ma, J., Taylor, R.H., Unberath, M. and Armand, M., 2021. Fluoroscopic navigation for a surgical robotic system including a continuum manipulator. IEEE Transactions on Biomedical Engineering, 69(1), pp.453-464.

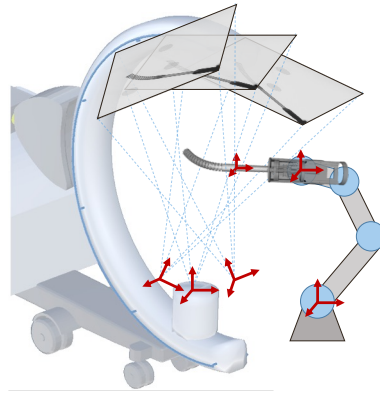
CM Registration Simulation Study



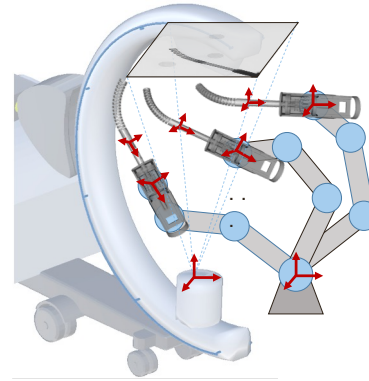
Single-view Registration



Multi-view Registration



Joint CM Registration



[20] Gao, C., Phalen, H., Sefati, S., Ma, J., Taylor, R.H., Unberath, M. and Armand, M., 2021. Fluoroscopic navigation for a surgical robotic system including a continuum manipulator. IEEE Transactions on Biomedical Engineering, 69(1), pp.453-464.



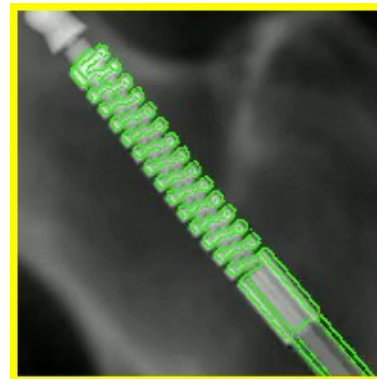
CM Registration Simulation Study



Single-view Registration



Simulated X-ray Image



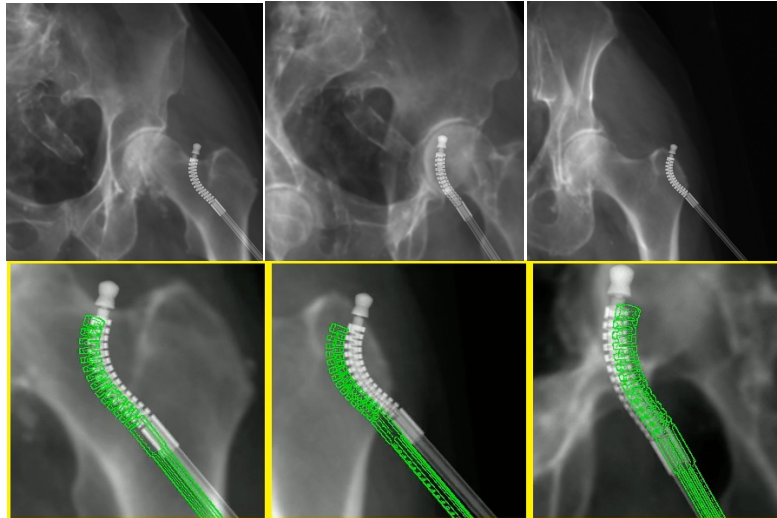
Registration Movie



CM Registration Simulation Study



Multi-view Registration

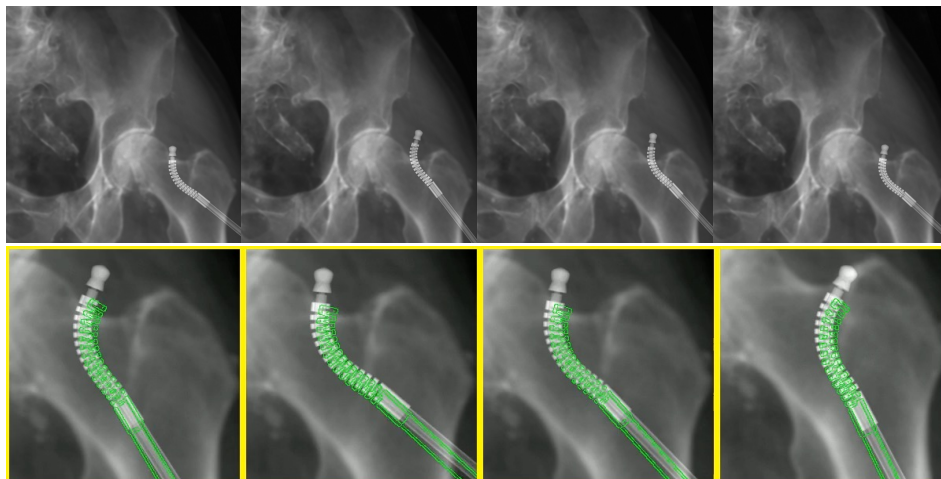


81

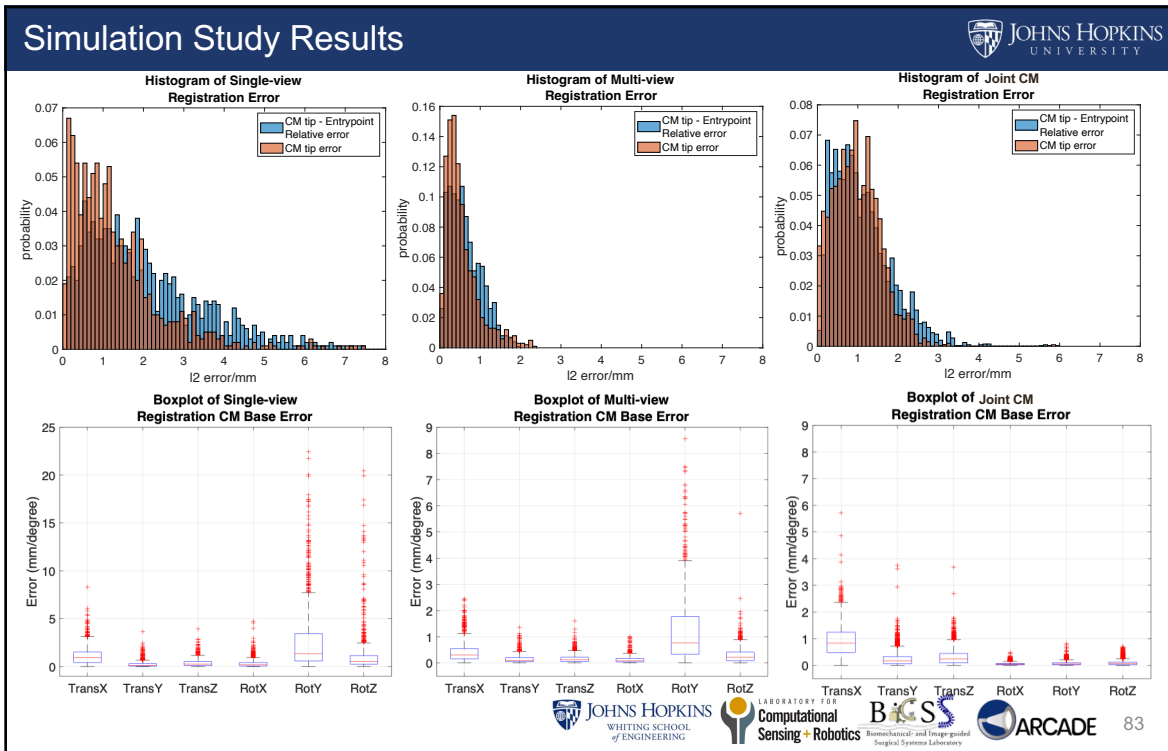
CM Registration Simulation Study



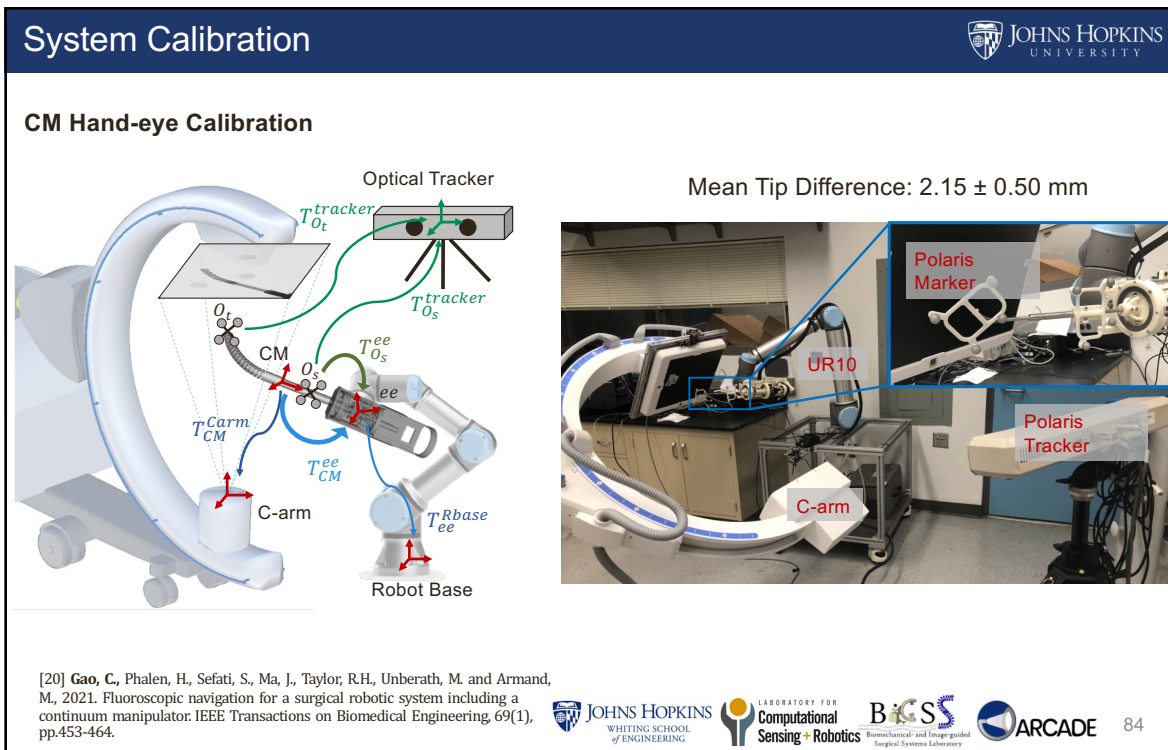
Joint CM Registration



82

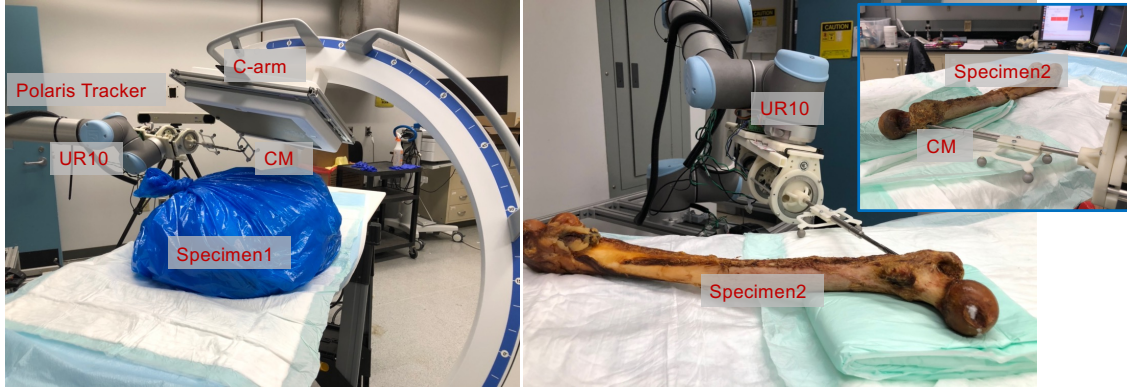


83



84

Core Decompression Cadaveric Experiment

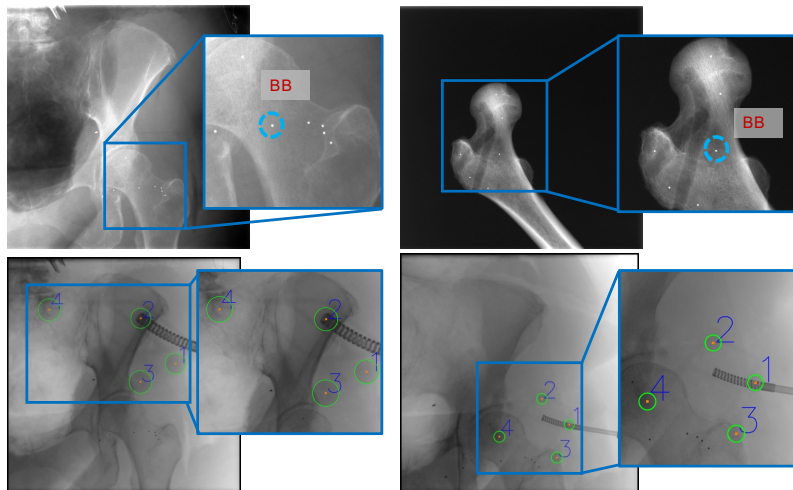


[20] Gao, C., Phalen, H., Sefati, S., Ma, J., Taylor, R.H., Unberath, M. and Armand, M., 2021. Fluoroscopic navigation for a surgical robotic system including a continuum manipulator. IEEE Transactions on Biomedical Engineering, 69(1), pp.453-464.

85

Core Decompression Cadaveric Experiment

Ground truth poses were obtained by solving a PnP problem using BB and fiducial landmarks



[20] Gao, C., Phalen, H., Sefati, S., Ma, J., Taylor, R.H., Unberath, M. and Armand, M., 2021. Fluoroscopic navigation for a surgical robotic system including a continuum manipulator. IEEE Transactions on Biomedical Engineering, 69(1), pp.453-464.

86

CM Cadaveric Experiment

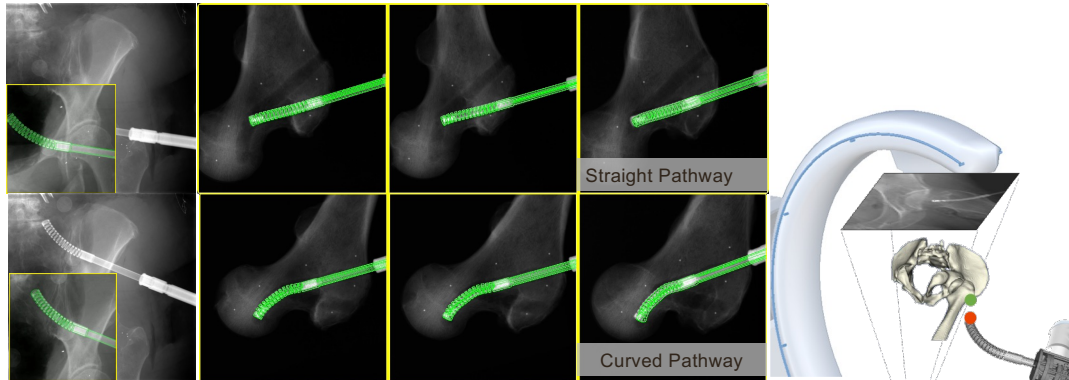


Table: CM Tip & Femur Entry Point Error^[12]

Trial ID	I	II	III	IV	V
CM Tip Position (mm)	2.73	2.44	2.77	4.20	2.09
Femur Entry Point (mm)	1.21	2.23	1.91	2.35	2.04
Relative (mm)	2.95	3.31	3.65	4.10	1.83

Femur entry point relative to CM tip
 Mean Error: 2.86 ± 0.80 mm

[20] Gao, C., Phalen, H., Sefati, S., Ma, J., Taylor, R.H., Unberath, M. and Armand, M., 2021. Fluoroscopic navigation for a surgical robotic system including a continuum manipulator. IEEE Transactions on Biomedical Engineering, 69(1), pp.453-464.



Conclusion and Contributions



Automatic Registration Pipeline

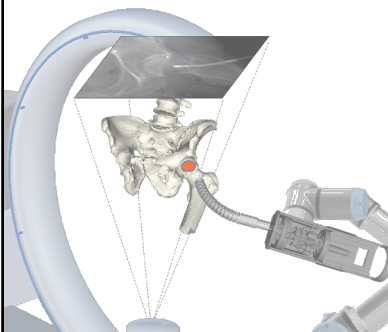
- A learning-based continuum manipulator detection method in X-ray images

Balanced Registration Ambiguity

- Jointly register multiple CM together and a modified hand-eye calibration method

System Validation

- Verified the the feasibility of applying purely fluoroscopic image-based registration for the CM navigation in simulation and cadaver experiments



Acknowledgment



Mr. Henry Phalen: Contributed to registration algorithm design, helped with the continuum manipulator calibration and cadaver experiments

Dr. Shahriar Sefati: Developed the continuum manipulator optical marker-based hand-eye calibration and control modules, helped with the system testing and algorithm design

Mr. Justin Ma: Developed the improved version of continuum manipulator

Related Publications/Manuscripts:

- **Gao, C.**, Phalen, H., Sefati, S., Ma, J., Taylor, R.H., Unberath, M. and Armand, M., 2021. Fluoroscopic navigation for a surgical robotic system including a continuum manipulator. IEEE Transactions on Biomedical Engineering, 69(1), pp.453-464. **Selected as a Featured Article**
- **C. Gao***, M. Unberath*, R. Taylor, & M. Armand (2019). Localizing dexterous surgical tools in X-ray for image-based navigation. IPCAI 2019 Long Abstract

* indicates joint first co-authors

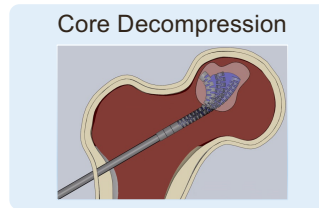
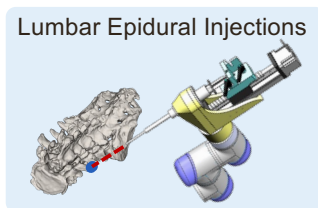
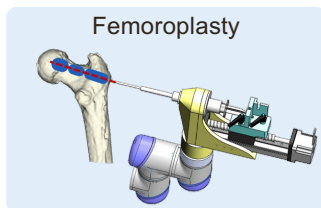


89

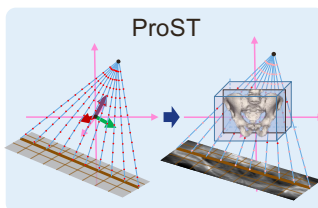
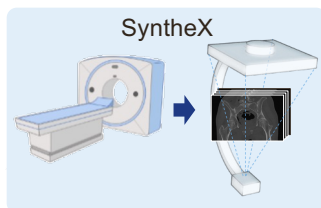
Introduction: Outline



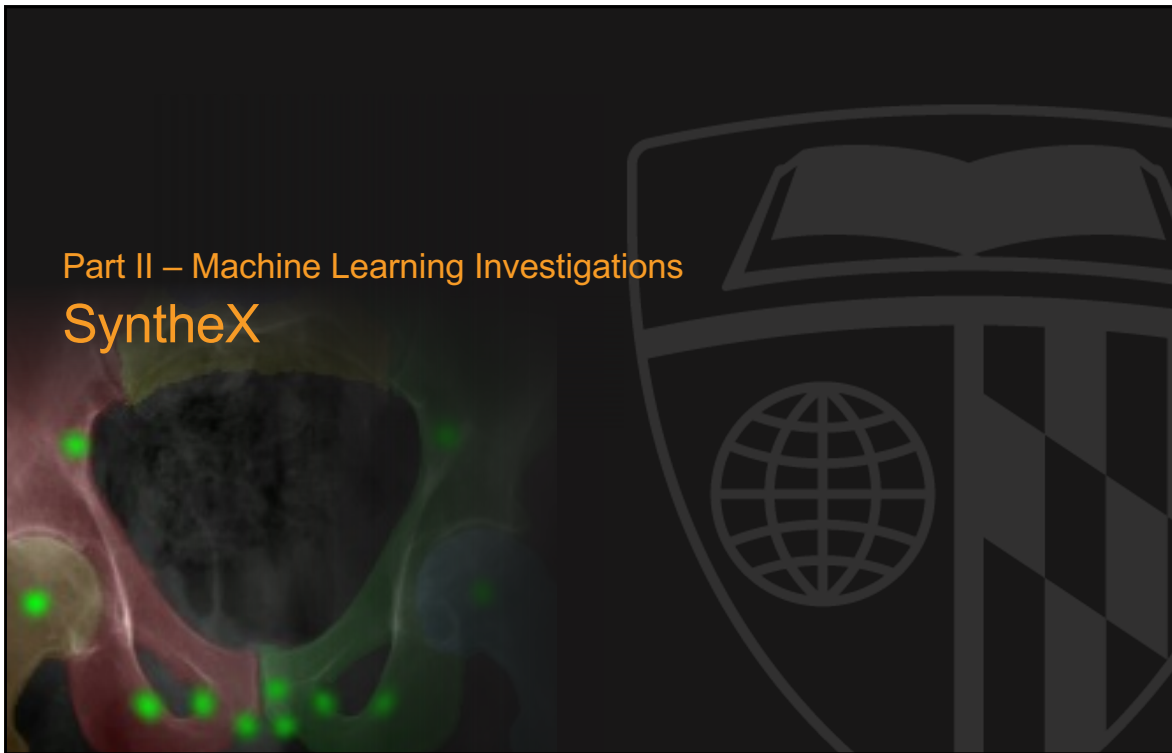
Part I: Clinical Application Development



Part II: Machine Learning Investigations



90

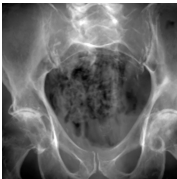


91

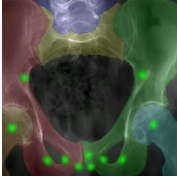
Recap JOHNS HOPKINS UNIVERSITY


Machine Learning X-ray Detection Tasks

- Automatic Registration Initialization

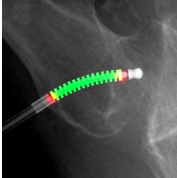


Pelvic Detection Network









CM Detection Network

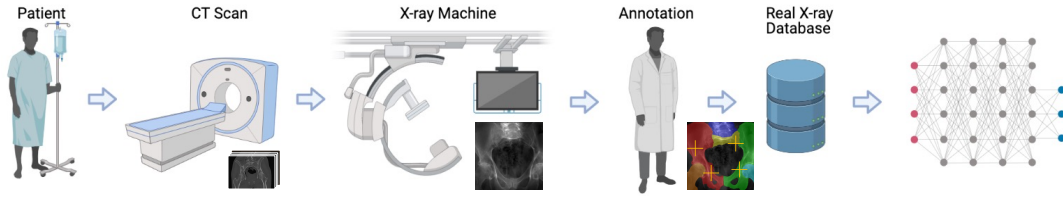


How do we generate training data?





92

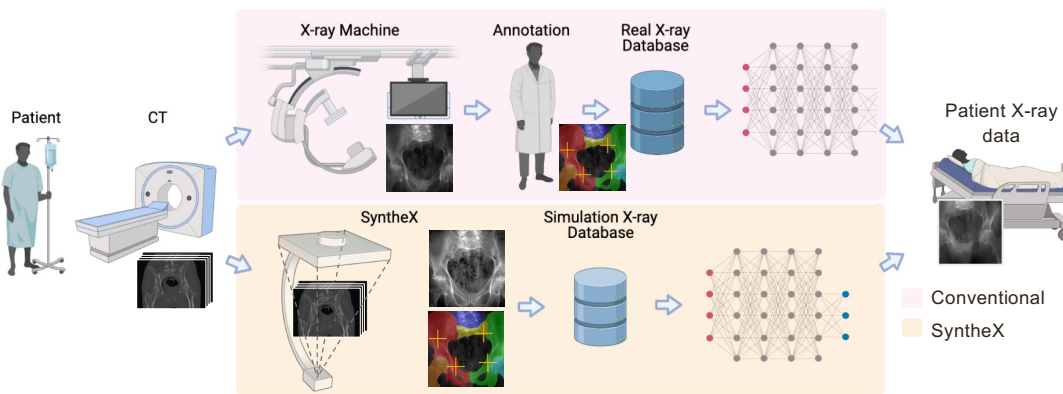
92

Motivation



SyntheX

SyntheX: Realistic Synthesis for X-ray Image Analysis



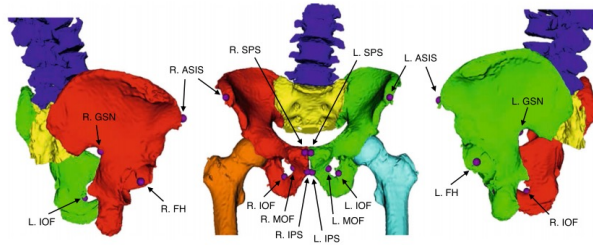
[21] Gao, C., Killeen, B.D., Hu, Y., Grupp, R.B., Taylor, R.H., Armand, M. and Unberath, M., 2022. SyntheX: Scaling Up Learning-based X-ray Image Analysis Through In Silico Experiments. Under Review of Nature Machine Intelligence

Unique Cadaveric Pelvic X-ray Dataset

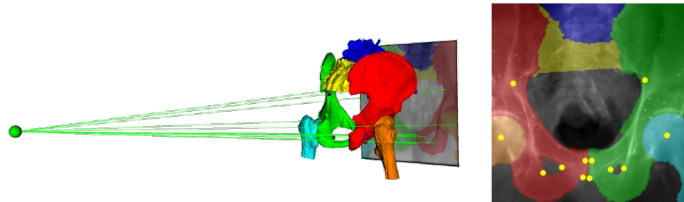


A cadaveric hip dataset^[22]

- 6 cadaveric specimens
- 366 X-ray images
- All have registered “ground truth” pose of corresponding CT scans



14 anatomical landmarks & 6 pelvic segmentations



Credit: Dr. Robert Grupp published this valuable dataset

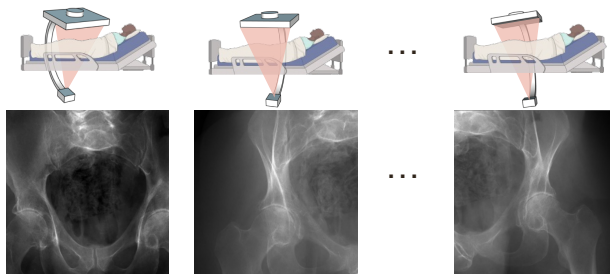
[22] Grupp, R. B., Unberath, M., Gao, C., Hegeman, R. A., Murphy, R. J., Alexander, C. P., ... & Taylor, R. H. (2020). Automatic annotation of hip anatomy in fluoroscopy for robust and efficient 2D/3D registration. *International journal of computer assisted radiology and surgery*, 15(5), 759-769.



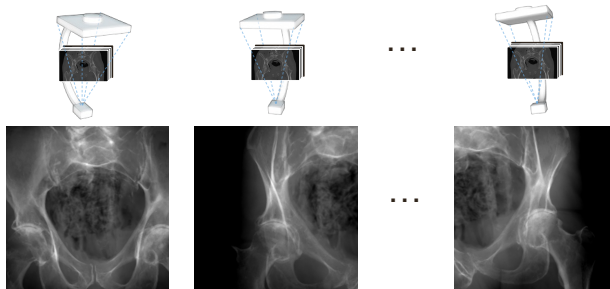
Precisely Matched Simulation-Real Database



Real X-ray Database



Simulation X-ray Database



Precisely Controlled Sim2Real Benchmark Experiments



Training

Testing

Sim2Real Techniques

- Domain Randomization
- Domain Adaptation
 - CycleGAN
 - Adversarial Discriminative Domain Adaptation

97

97

Concurrent Segmentation and Landmark Detection



Hip Imaging Downstream Task

→ Conv2d + ReLU

→ (Conv2d + ReLU) × 2 + MaxPooling

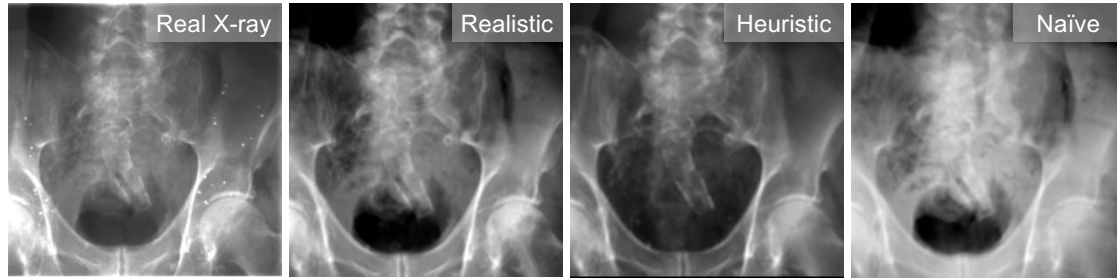
→ ConvTranspose2d + (Conv2d + ReLU) × 2

98

98

[10] Grupp, R.B., Unberath, M., Gao, C., Hegeman, R.A., Murphy, R.J., Alexander, C.P., Otake, Y., McArthur, B.A., Armand, M. and Taylor, R.H., 2020. Automatic annotation of hip anatomy in fluoroscopy for robust and efficient 2D/3D registration. International journal of computer assisted radiology and surgery, 15(5), pp.759-769.

Ablation Simulators



DeepDRR^[23]

- 3D Organ Segmentation
- Specified Attenuation
- Photon Spectrum
- Noise Sampling and Scattering

Xreg DRR^[24]

- Simple Thresholding
- Noise Sampling

Naïve DRR

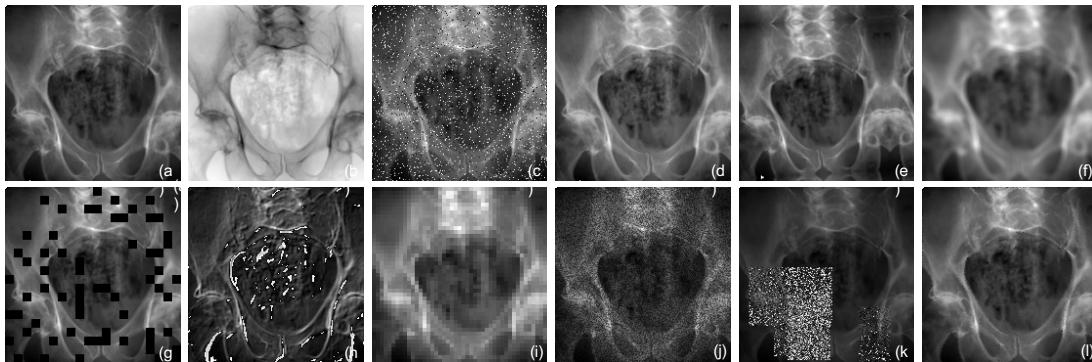
- Only line integration

[23] Unberath, M., Zaech, J.N., Lee, S.C., Bier, B., Fotouhi, J., Armand, M. and Navab, N., 2018, September. DeepDRR—a catalyst for machine learning in fluoroscopy-guided procedures. In International Conference on Medical Image Computing and Computer-Assisted Intervention (pp. 98-106). Springer, Cham.

[24] <https://github.com/rg2/xreg>

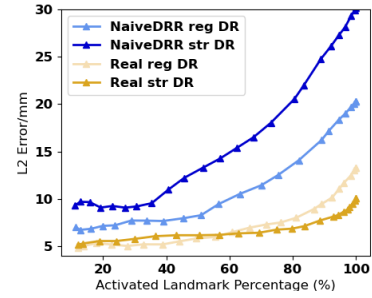
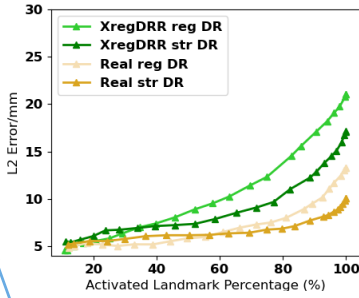
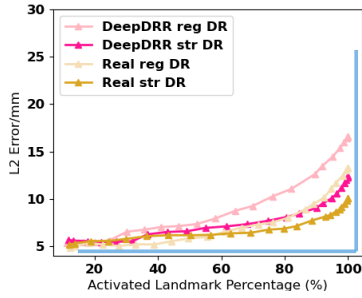
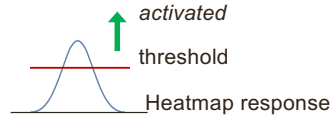
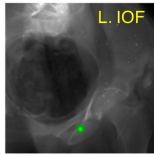
Domain Randomization

- Regular DR: Gaussian noise; Contrast; Random Crop
- Strong DR:



(a) No DR. (b) Inverting. (c) Pepper and salt noise injection. (d) Contrast. (e) Affine transform. (f) Blurring. (g) Dropout. (h) Sharpening and embossing. (i) Pooling. (j) Element-wise multiplication. (k) Box corruption. (l) Elastic effect.

Landmark Detection Result – Domain Randomization

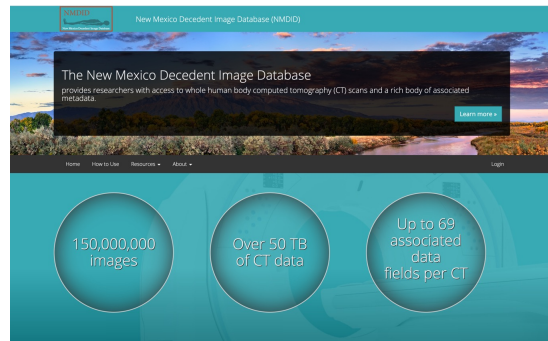


Ideal Curve

101

Scaled-up Simulation

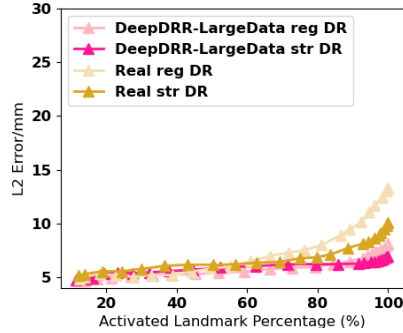
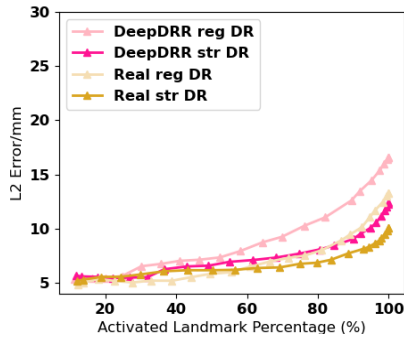
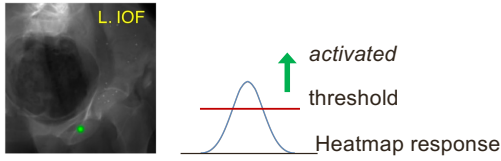
- Annotated 20 CT scans from the New Mexico Decedent Image Database^[24]
- Simulate 10k X-rays
- More sampled geometries



[24] Edgar, JH; Daneshvari Berry, S; Moes, E; Adolphi, NL; Bridges, P; Nolte, KB (2020). New Mexico Decedent Image Database. Office of the Medical Investigator, University of New Mexico. doi.org/10.25827/5s8c-n515.

102

Landmark Detection Result – Scaled Up

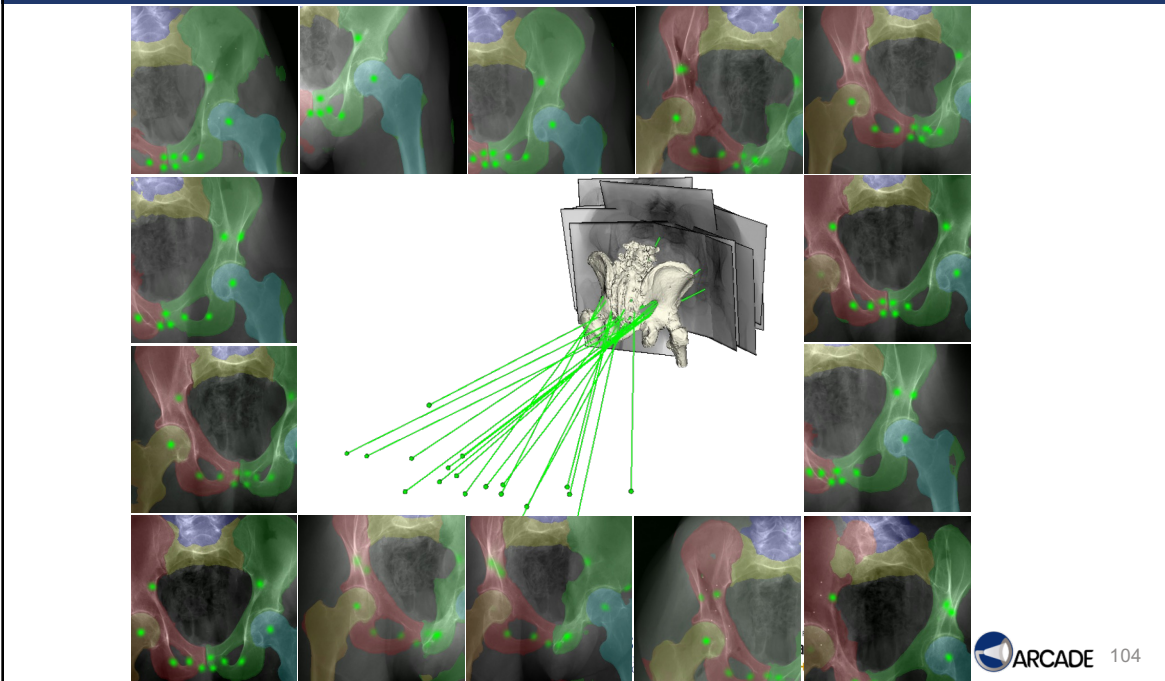


Scaled-up simulation training outperforms Real2Real!



103

Qualitative Results of Sim2Real Detection Results



104

Surgical Tool Detection Downstream Task

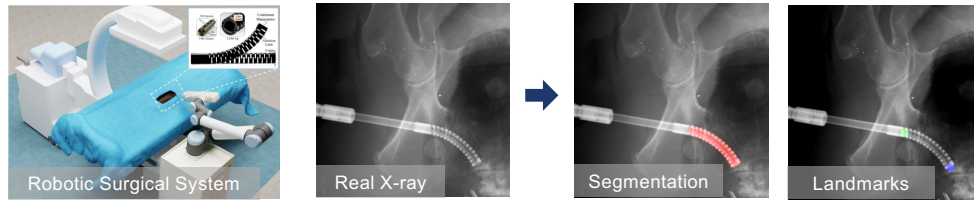


Table: Detection Accuracy

	Landmark Error (mm)	Dice Score
<i>Sim2Real</i>	2.13 ± 2.27	0.860 ± 0.115
<i>Real2Real</i>	1.90 ± 5.49	0.406 ± 0.194

- Real2Real was trained on 200 annotated X-ray images, Sim2Real was trained using 20k synthetic images

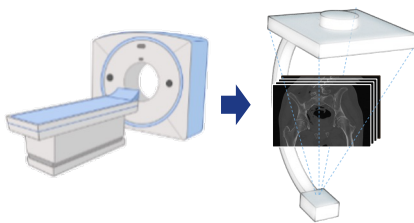


105

Conclusion and Contributions



- We **quantified the role of domain shift** in the deterioration of machine learning model performance from training in simulation to deployment on real data
- Physics-based Realistic Simulation with DR generalizes the best. Scaling up simulation dataset even outperforms Real2Real.
- SyntheX as a promising alternative for machine learning X-ray imaging tasks



106

Acknowledgment



Mr. Benjamin Killeen: Contributed to comparison experiment running

Mr. Yicheng Hu: Contributed to simulation geometry calibration and experiment running

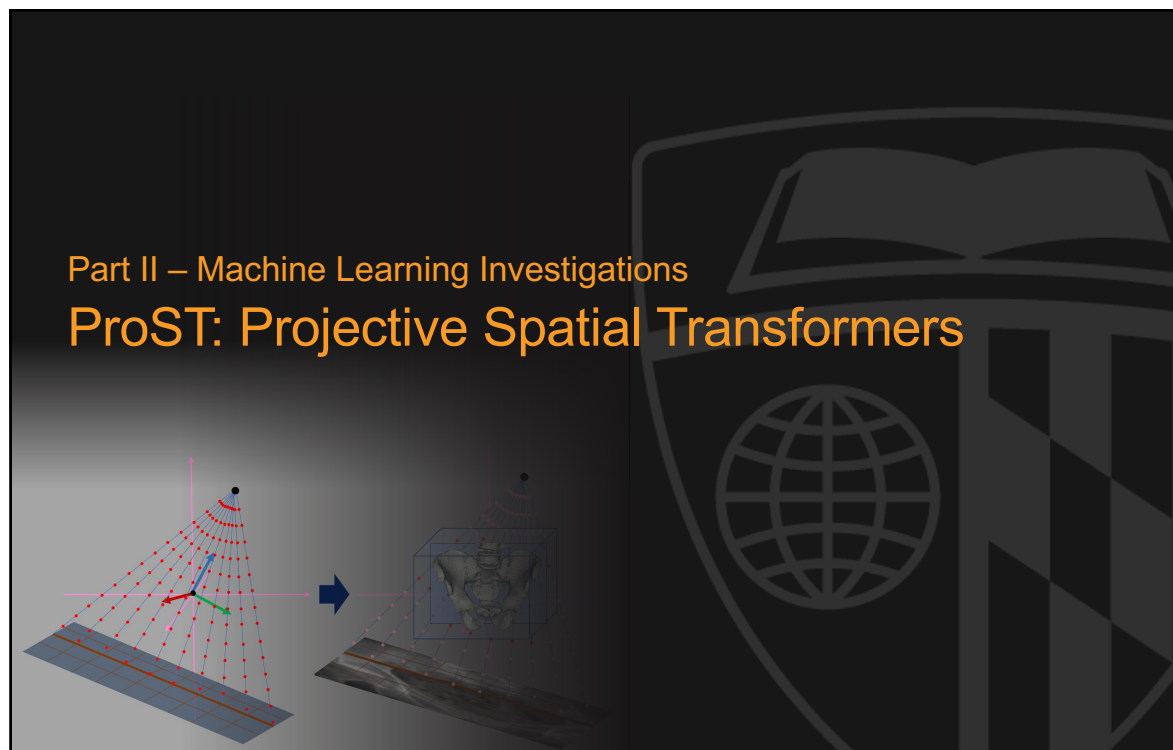
Dr. Robert Grupp: Collected and published the pelvic dataset

Related Publications/Manuscripts:

- **Gao, C.**, Killeen, B.D., Hu, Y., Grupp, R.B., Taylor, R.H., Armand, M. and Unberath, M., 2022. SyntheX: Scaling Up Learning-based X-ray Image Analysis Through In Silico Experiments. Under Review of Nature Machine Intelligence



107

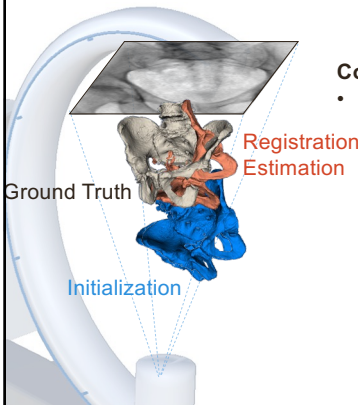
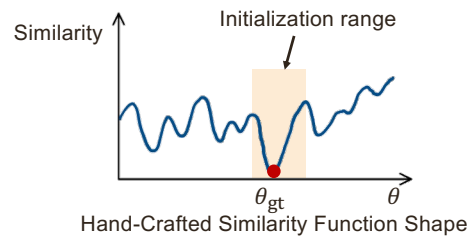


108

Recap: 2D/3D Registration Challenge

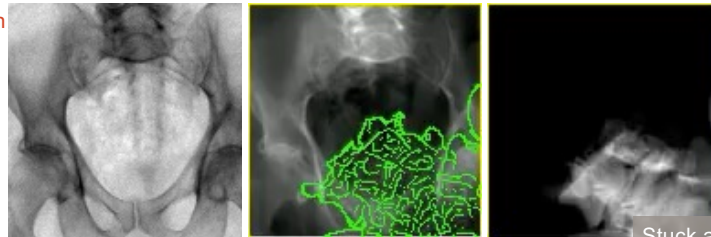
Narrow Capture Range

- Local minima of conventional hand-crafted similarity function, such as Grad-NCC
- Requires the initialization close to the ground truth



Conventional Intensity-based 2D/3D Registration Strategy:

- CMAES + Patch-based Grad-NCC^[25]



Stuck at a local minimum!

[25] Grupp, R.B., Armand, M. and Taylor, R.H., 2018. Patch-based image similarity for intraoperative 2D/3D pelvis registration during periacetabular osteotomy. In CARE Workshop of MICCAI 2018.

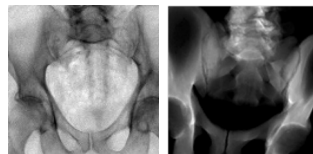
109

Related Work

Pose Regression Methods

Limitations:

- Learning a mapping function from 2D projections is an **ill-posed problem**, which is prone to **strongly overfit to training domain**
- **Direct pose regression is unconstrained**, which can change dramatically if the input image appearance has a tiny difference



High-level Prototype

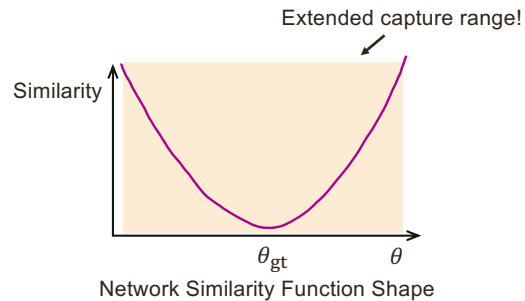
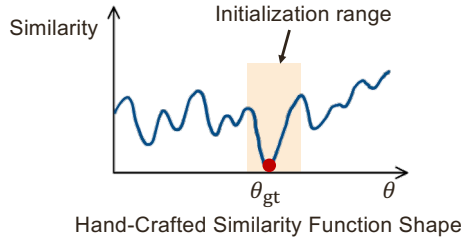
[26] Miao, S., Wang, Z., and Liao, R., 2016. A CNN regression approach for real-time 2D/3D registration. IEEE transactions on medical imaging, 35(5), pp.1352-1363.

110

Motivation

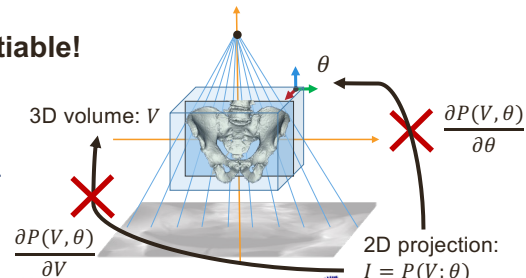


A More Desired Solution



Traditional DRR Projector is not Differentiable!

- Oversized system matrix $A(\theta)$ to fit in memory
- Conventional optimization strategies are numeric-based methods, such as CMAES



[27] Hansen, N., Müller, S.D. and Koumoutsakos, P., 2003. Reducing the time complexity of the derandomized evolution strategy with covariance matrix adaptation (CMA-ES). Evolutionary computation, 11(1), pp.1-18.



111

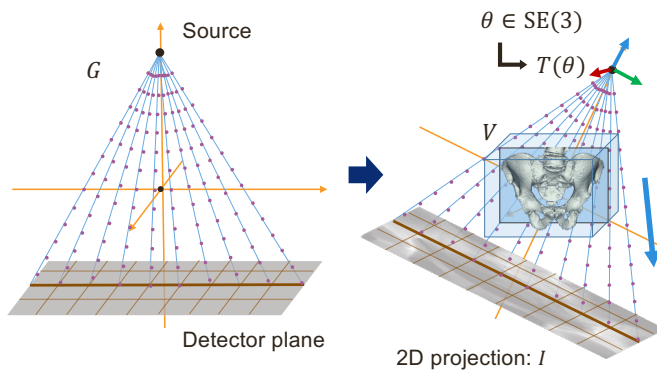
Projective Spatial Transformers (ProST)



ProST -- Differentiable DRR Operator

Spatial Sampling Grid: G

- Follows projection geometry



Given a pose parameter θ and 3D volume V as input, the DRR projection is:

$$I = P(V, \theta) = \text{sum}(\text{interp}(V, T(\theta)G))$$

↓ Summation along the projection direction
↓ Linear transformation
↓ Linear interpolation

Breakthrough:

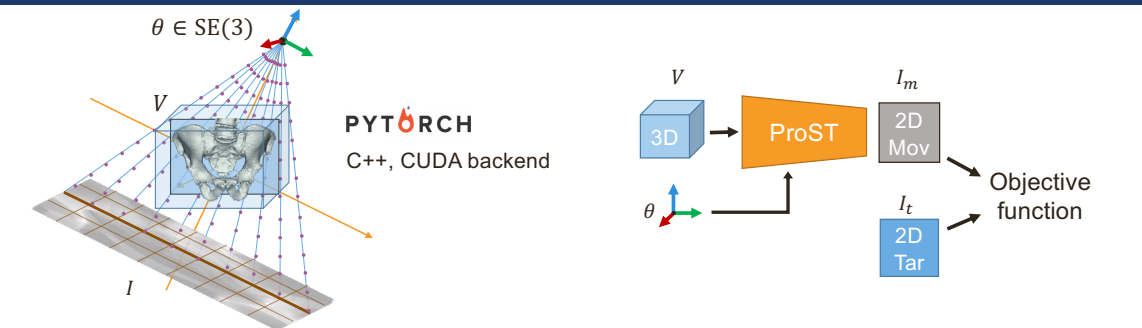
$\frac{\partial P(V, \theta)}{\partial \theta}$ $\frac{\partial P(V, \theta)}{\partial V}$ are differentiable!


[28] Gao, C., Liu, X., Gu, W., Killeen, B., Armand, M., Taylor, R., & Unberath, M. (2020, October). Generalizing spatial transformers to projective geometry with applications to 2D/3D registration. In International Conference on Medical Image Computing and Computer-Assisted Intervention (pp. 329-339). Springer, Cham.

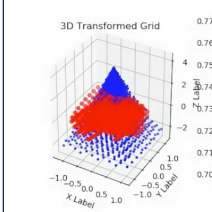


112

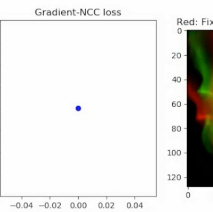
Projective Spatial Transformers (ProST)



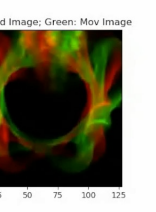




3D Transformed Grid



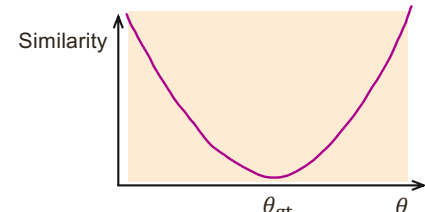
Gradient-NCC loss







Red: Fixed Image, Green: Mov Image

Example registration using Grad-NCC similarity, optimized by PyTorch built-in SGD optimizer

How do we learn a better similarity function?




Network Similarity Function Shape





113

113

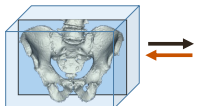
ProST 2D/3D Registration Pipeline



Target Similarity Function -- Geodesic Loss


- A convex objective function with respect to SE(3) pose parameters

CT Segmentation




3D CNN

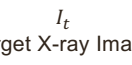
ProST




Moving Image



Target X-ray Image



CrossViT







Predicted Similarity S_{net}

Gradient-driven Double Backward Loss

Geodesic Gradient

$$\frac{\partial S_{net}}{\partial \theta_m}$$

$$\frac{\partial L_{geo}}{\partial \theta_m}$$

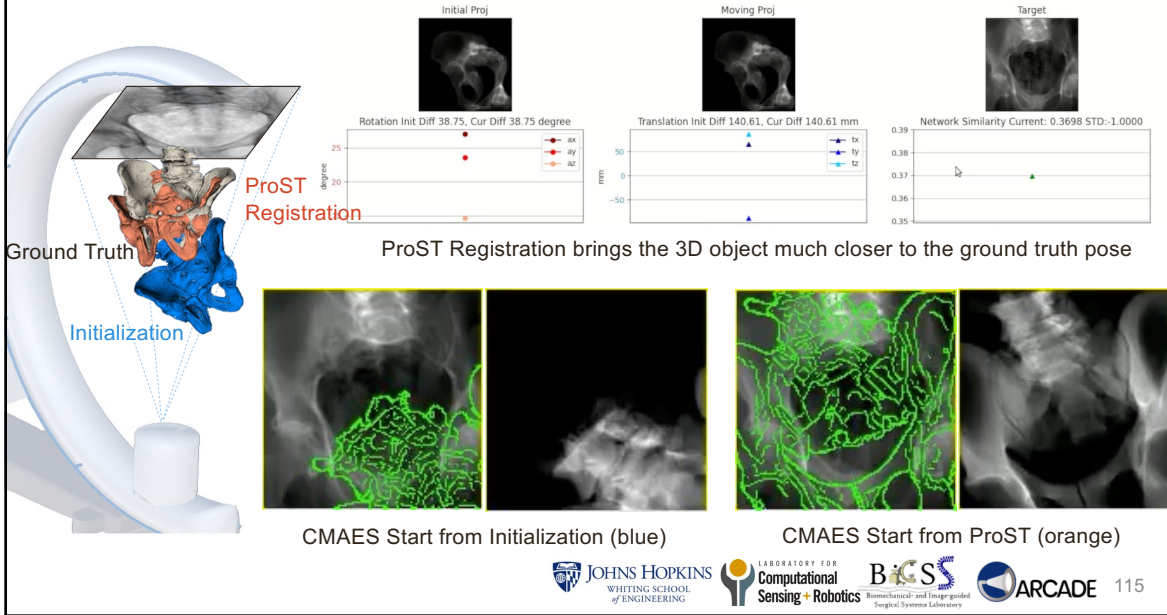




114

114

Example Registration using ProST Architecture



ProST Registration using Learned Similarity Function

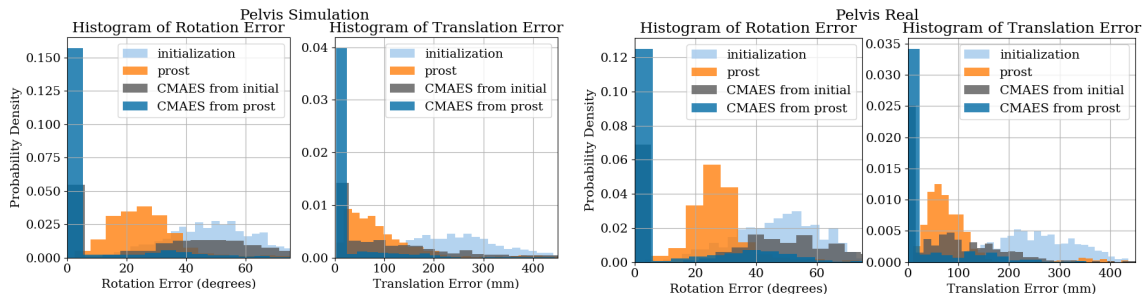


115

Experiments and Results



- Our pipeline was trained using 19 CT scans, evaluated on 1,000 synthetic X-rays and 200 real X-rays



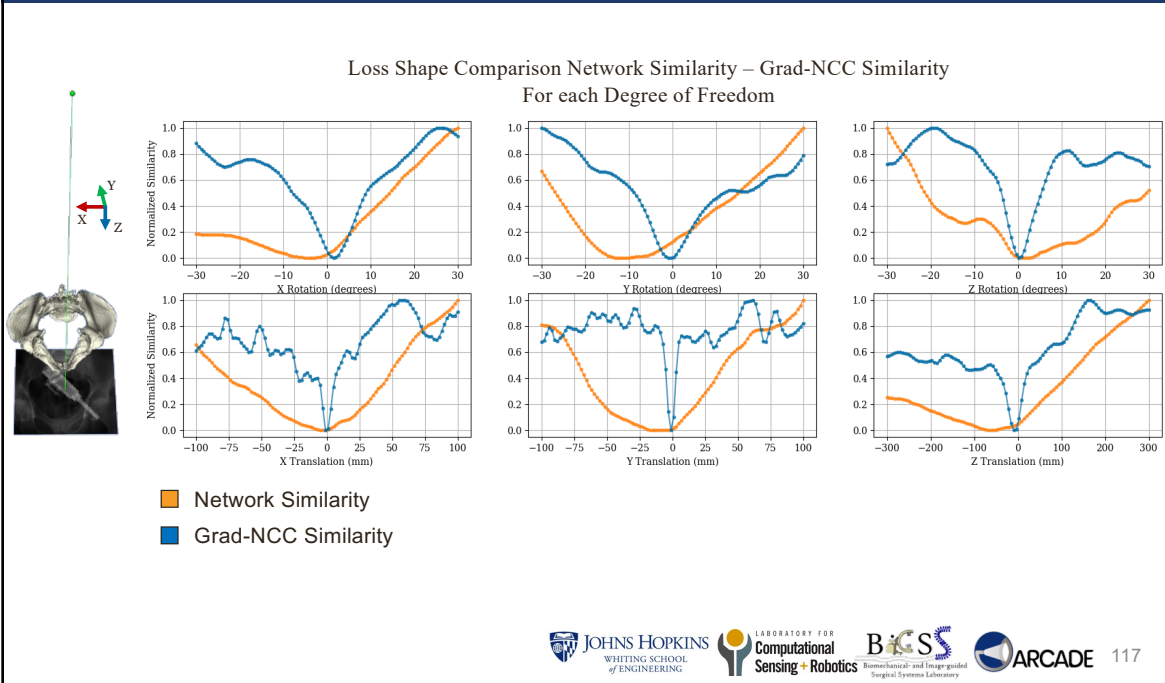
Success Rate (%): Mean Target Registration Error < 10 mm

	Simulation	Real
CMAES from Initialization	32.6	36.0
CMAES from ProST Registration	82.6	73.2



116

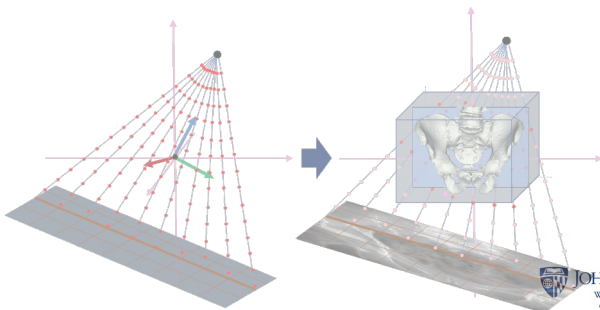
Experiments and Results



117

Conclusion & Contributions

- A novel ProST module, which enables differentiable volumetric rendering of X-ray images using CT volumes and analytical gradient calculation with respect to pose parameters.
- An innovative end-to-end 2D/3D image registration by learning a convex-shape similarity function.
- Demonstrated that ProST registration largely extends the conventional CMAES registration capture range.



118

Acknowledgment



Dr. Xingtong Liu: Contributed to ProST design, registration architecture design, and double backward loss.

Ms. Anqi Feng: Contributed to data processing and comparison experiments in extended journal submission

Mr. Wenhao Gu and Mr. Benjamin Killeen: Provided valuable suggestions

Related Publications/Manuscripts:

- **Gao, C.**, Liu, X., Gu, W., Killeen, B., Armand, M., Taylor, R., & Unberath, M. (2020, October). Generalizing spatial transformers to projective geometry with applications to 2D/3D registration. In International Conference on Medical Image Computing and Computer-Assisted Intervention (pp. 329-339). Springer, Cham.
- **Gao, C.**, Feng, A., Liu, X., Taylor, R.H., Armand, M. and Unberath, M., 2022. A Fully Differentiable Framework for 2D/3D Registration and the Projective Spatial Transformers. Ready in submission to TMI



119

Summary, Future Work Outlook and Acknowledgment

120

Summary

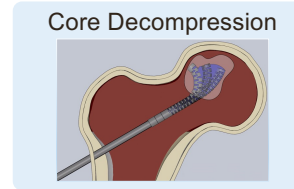
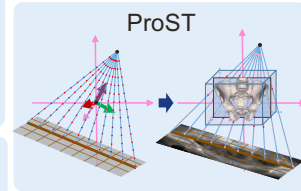
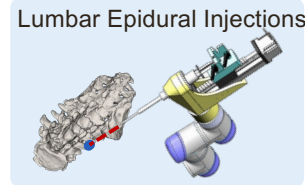
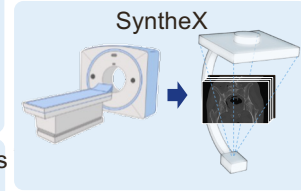
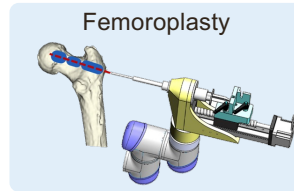
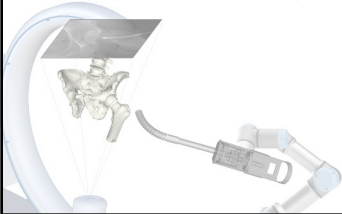


Effective Navigation System

- Use purely fluoroscopic images
- (Semi-) Automatic registration algorithms
- Robot system-level validation
- Feasibility on variant clinical applications

Novel AI Frameworks

- Benefit machine learning X-ray imaging research
- Provide solutions to solve fundamental registration challenges



121

Future Work Outlook



Optimal C-arm view geometry

- The best view that the registration has the highest chance to succeed

Patient Motion Verification

- Automatically detect patient motion and correct registration

Registration Uncertainty

- Confidence of the registration pose estimations

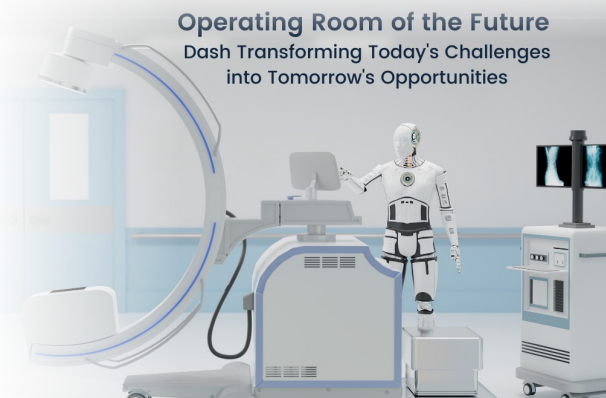


Image from <https://dashtechinc.com/operating-room-of-the-future-dash-transforming-todays-challenges-into-tomorrows-opportunities/>



122

Thank you!

